THESIS FOR THE DEGREE OF DOCTOR OF PHILOSOPHY

Quality Assurance and Regulatory Frameworks for Hyperthermia Therapy

Mattia De Lazzari

Department of Electrical Engineering
Chalmers University of Technology
Gothenburg, Sweden, 2025

Quality Assurance and Regulatory Frameworks for Hyperthermia Therapy

Mattia De Lazzari
ISBN 978-91-8103-337-3

Acknowledgements, dedications, and similar personal statements in this thesis, reflect the author's own views.

Selected material from the author's licentiate thesis: Mattia De Lazzari, "Practical Implementation of Quality Assurance Guidelines for Hyperthermia Therapy", Gothenburg, Sweden, Dec. 2023, is republished in this Ph.D. thesis.

Doktorsavhandlingar vid Chalmers tekniska högskola
Ny serie nr 5794
ISSN 0346-718X
DOI https://doi.org/10.63959/chalmers.dt/5794

Department of Electrical Engineering
Chalmers University of Technology
SE-412 96 Gothenburg, Sweden
Phone: +46 (0)31 772 1000

Cover:
Representation of the quality assurance (QA) procedure in hyperthermia. After application of the derived corrections, the actual focus is accurately aligned with the intended target location (dashed lines).

Printed by Chalmers Digital Printing
Gothenburg, Sweden, December 2025

Abstract

Hyperthermia (HT) has shown to be a powerful enhancer of chemotherapy and radiotherapy in numerous clinical trials. Its therapeutic effectiveness depends on the thermal dose delivered, which is determined by the quality and consistency of the applied heating. Quality Assurance (QA) guidelines ensure that HT devices deliver heat in a controlled, safe, and reproducible manner.

However, translation of QA guidelines into routine clinical practice has been limited by the lack of suitable tools and the lack of practical implementation guidance. This thesis addresses these gaps by (i) developing new phantoms for HT QA and (ii) demonstrating the application of the latest QA guidelines for both superficial (SHT) and deep HT (DHT).

For SHT applications, a novel fat-mimicking phantom was developed using an ethylcellulose-stabilized glycerol-in-oil emulsion. This material exhibited dielectric and thermal properties representative of fat tissue, with acceptable variability across the frequency range relevant for HT. Subsequently, it was applied in the QA evaluation of the SHT Lucite Cone Applicator (LCA), following the quality metrics defined in current HT guidelines. This experience provided practical insight into the implementation of guidelines in the clinical environment.

For DHT, the phantom design was optimised, supported by computational studies, to represent different anatomical areas. These phantoms were then used in a multi-institutional QA comparative study involving six European HT centres, in which the heating and focusing ability of clinically used DHT devices was evaluated. The study also revealed several practical challenges in QA implementation, including experimental setup, probe calibration, procedure duration, and the definition of suitable quality metrics. These findings directly contributed to the development of the latest QA guidelines for deep HT and support their integration into routine clinical practice.

Finally, the relationship between QA guidelines and the EU Medical Devices Regulation (MDR) regulatory framework was clarified using an in-house developed phased-array radiative applicator as a case study, outlining key steps from preliminary investigation to system verification and validation.

Keywords: Hyperthermia, Quality Assurance, Phantoms, Thermal Dosimetry, MDR.

To my family.

List of Publications

This thesis is based on the following publications:

[A] **Mattia De Lazzari**, Anna Ström, Laura Farina, Nuno P Silva, Sergio Curto, Hana Dobšíček Trefná , "Ethylcellulose-stabilized fat-tissue phantom for quality assurance in clinical hyperthermia". Published in International Journal of Hyperthermia, May. 2023.

[B] **Mattia De Lazzari**, Hana Dobšícek Trefná, Carolina Carrapiço-Seabra, Patrick V. Granton, Sergio Curto, Dario B. Rodrigues, "Quality Assurance Phantoms for Deep Hyperthermia Devices: Design Principles Informed by Computational Modeling". Submitted to Physics in Medicine and Biology.

[C] Carolina Carrapiço-Seabra*, **Mattia De Lazzari***, Abdelali Ameziane, Gerard C. van Rhoon, Hana Dobšícek Trefná, Sergio Curto, "Application of the ESHO-QA guidelines for determining the performance of the LCA superficial hyperthermia heating system". Published in International Journal of Hyperthermia, Oct. 2023.

[D] **Mattia De Lazzari***, Carolina Carrapiço-Seabra*, Dietmar Marder, Gerard C. van Rhoon, Sergio Curto, Hana Dobšícek Trefná, "Toward enhanced quality assurance guidelines for deep hyperthermia devices: a multi-institution study". Published in International Journal of Hyperthermia, Nov. 2024.

[E] **Mattia De Lazzari**, Anton Rink, Patrick V. Granton, Dario B. Rodrigues, Hana Dobšícek Trefná, "Navigating EU MDR 2017/745 for in-house deep hyperthermia systems: A practical workflow and case study". To be submitted to IEEE Journal of Translational Engineering in Health and Medicine.

Other publications by the author, not included in this thesis, are:

[F] Hana Dobšíček Trefná, Hans Crezee, Dietmar Marder, **Mattia De Lazzari**, Carolina Carrapico Seabra, Marianne Göger-Neff, Remko Zweije, Manfred Schmidt, Sultan Abdel-Rahman, Gerard van Rhoon, H. Petra Kok, Sergio C. Curto, Dario B. Rodrigues, "Quality Assurance Guidelines for Performance

*Shared first authorship

Assessment of Phased-Array Deep Hyperthermia Therapy Systems". Submitted to International Journal of Hyperthermia, 2025.

[G] **Mattia De Lazzari**, Wojtek Napieralski, Thien Nguyen, Anna Ström, Hana Dobšíček Trefná, "Design and manufacture procedures of phantoms for hyperthermia QA guidelines". *Proc. 17th European Conference on Antennas and Propagation (EuCap)*, Florence, Mar. 2023.

[H] **Mattia De Lazzari**, Fredrik Lorentzon, Anna Ström, Hana Dobšíček Trefná, "An EC-based oleogel fat-phantom for Quality Assurance procedures". *13th International Congress of Hyperthermic Oncology (ICHO)*, Digital, Oct. 2021.

[I] **Mattia De Lazzari**, Martin Wadepohl, Hana Dobšíček Trefná, "Hyperthermia system development in the perspective of the European Medical Devices Regulation". *34th Annual Meeting European Society for Hyperthermic Oncology (ESHO)*, Göteborg, Sept. 2022.

[J] **Mattia De Lazzari**, Dario Rodrigues, Sergio Curto, Carolina C. Seabra, Dietmar Marder, Hana Dobšíček Trefná, "Supporting the design of QA phantoms for deep hyperthermia devices". *35th Annual Meeting European Society for Hyperthermic Oncology (ESHO)*, Köln, Sept. 2023.

[K] **Mattia De Lazzari**, Carolina C. Seabra, Dietmar Marder, Sergio Curto, Hana Dobšíček Trefná, "Design of a multi-institutional study on Deep Hyperthermia QA assessment". *35th Annual Meeting European Society for Hyperthermic Oncology (ESHO)*, Köln, Sept. 2023.

[L] Dario Rodrigues, **Mattia De Lazzari**, Carolina C. Seabra, Ulf Lamprecht, Manfred Schmidt, Dietmar Marder, Sergio Curto, Hana Dobšíček Trefná, Jason K. Molitoris, "Numerical feasibility of delivering deep hyperthermia to lateral tumors opposite to metallic hip implants". *39th Annual Society for Thermal Medicine (STM) Meeting*, Houston, May. 2024.

[M] **Mattia De Lazzari**, Rüdiger Wessalowski, Oliver Mils, Udo Kontny, Beate Timmermann, Ronald Richter, Hana Dobšíček Trefná, "Biological modeling shows thermal enhancement of radiation dose in a pediatric sarcoma patient treated with proton beam therapy and regional deep hyperthermia".

36th Annual Meeting European Society for Hyperthermic Oncology (ESHO), Malaga, Nov. 2024.

[N] **Mattia De Lazzari**,Dario Rodrigues, Carolina C. Seabra, Sergio Curto, Hana Dobšíček Trefná, "Evaluation of thermal mapping accuracy in clinical hyperthermia using QA phantoms". *14th International Congress of Hyperthermic Oncology (ICHO)*, Seoul, Sept. 2025.

[O] Robin Nilsson, **Mattia De Lazzari**, Isabella Sykkö, Anna Bäck, Hana Dobšíček Trefná, "Microwave hyperthermia for brain lesions: thermal coverage analysis in realistic clinical scenarios". *14th International Congress of Hyperthermic Oncology (ICHO)*, Seoul, Sept. 2025.

Contents

Acknowledgments

This five-year journey would not have been possible without the support, friendship, and love of the many people I was fortunate enough to meet during my PhD. Each of you, in your own way, made this journey unique and helped me build a new home, far from home.

First of all, I would like to express my deepest gratitude to my supervisor, Prof. Hana Dobšíček Trefná. You have supported me with patience since the very first day, and you always brought me back onto the right path whenever I doubted myself. And it is indeed true: *allt kommer att lösa sig!*

Additionally, I would like to thank my co-supervisor, Prof. Dario Rodrigues, for his guidance, his always attentive and precise feedback, and for welcoming me to the "Charm City".

I would also like to thank all my colleagues, past and present, from the Biomedical Electromagnetics group: Laura, Moein, Robin, August, Max, Andreas, Xuezhi, and Mikael. A special acknowledgment goes to Laura and Moein for being exceptional friends, for supporting each other, and for supporting me whenever you saw me walking into your office (and wondering when I was going to leave). Thank you, Robin, for sharing part of this hyperthermia journey with me—discussing ideas, finding solutions together, and for keeping track of the number of coffee cups on my desk. I also extend my appreciation to the Biomedical Signal Processing group, and in particular to Anna, for the mutual support during this final stretch of our PhDs.

There are many other people at Chalmers (or connected to the Chalmers sphere) whom I had the pleasure of getting to know better outside the intricate corridors of EDIT. Thank you all for sharing so many enjoyable moments and, for many of you, for becoming dear friends: thank you Gabriel, Alvin, Stephie, Alejandra, Rita, Erik, Ying, Ola, Yara, André, Boss, Nishant, Nanami, Tao, Sherry, Kilian, Rikard, and Sabino for the countless activities and memories we shared together. Thank you to Martina, Francesco, Chiara, and Michela for making me feel closer to home, and also to Delio and André, Italians by adoption by now. Thanks as well to Albert for your friendship and always timely suggestions, to Attila—always ready for a hike—and to Ahmet, Godwin, and Faris. A special thanks also to the remaining fifth-floor people—Isac, Filip, Adam, Lasse, Daniel, Lorenzo, and Kristian—for the cheerful moments during work breaks and after-work gatherings. Thank you, Lluc, for all the fikas spent discussing life.

I sincerely thank my friends here in Göteborg, as well as those who have left the city but remain close through their invaluable friendship: thank you Anna, Arman, Hampus, Brett, Hans, Alexia, Henry, Dana, Chiara, and Lucas. Thank you for being, after all this time, such wonderful friends.

A big thank you to my friends dispersed across Europe: Lukas, Loïc, João, Matteo, Ben, and Carolina. We spent only one semester together, but it felt like we had known each other forever. Thank you also, Ivan for your friendship (and to Victor's Café for our uncountable brunches).

I would also like to thank all the fellow ESRs of the HyperBoost consortium for sharing so many memorable moments around Europe. In particular, I would like to thank the Erlangen duo, Rupali and Azzaya; our electromagnetics (and selfie) expert, Faezeh; the Spanish-speaking trio Timo, Fernando, and Sergio; our biologist, Priyanshu; and our super efficient Adela. Above all, I want to express my biggest thank you to Carolina, for everything we did together to reach this milestone. Our collaboration was truly fruitful and grew into a friendship. Thank you for all of this (*andiamo!*).

To my friends back in Italy, a special thank you—especially to my dear friends Davide and Elisabetta: distance has not diminished our connection. Thank you also to Edoardo, Giorgia, Andrea, Elia, Elisa, and Teresa for being close from our university days until today.

I feel immense gratitude toward my family for their unwavering support and love. I could not have made it this far without you. Grazie mamma, papà, Marco, Ale, zie, zii e nonni. Vi voglio bene.

Finally, I want to thank you, Aurélien, for being by my side during the last part of this journey. You made it special.

Mattia, Göteborg, December 2025

Acronyms

CT: Computed Tomography

DHT: Deep Hyperthermia

EC: Ethylcellulose

EM: Electromagnetic

EMF: Electromagnetic Field

EFS: Effective Field Size

ESHO: European Society for Hyperthermic Oncology

HT: Hyperthermia

H&N: Head and Neck

IR: Infrared

ISO: International Organization for Standardization

LCA: Lucite Cone Applicator

MDR: Medical Device Regulation

MR: Magnetic Resonance

QA: Quality Assurance

RF: Radiofrequency

RT: Radiotherapy

SAR: Specific Absorption Rate

SHT: Superficial Hyperthermia

TEFS: Thermal Effective Field Size

TEFV: Thermal Effective Field Volume

TEPD: Thermal Effective Penetration Depth

TR: Temperature Rise

VNA: Vector Network Analyzer

WPP: Wallpaper Paste

Part I

Overview

CHAPTER 1

Introduction

Cancer is reported by the World Health Organization (WHO) as a prominent global cause of death, responsible for approximately 10 million fatalities in the year 2022 [1]. The umbrella term encompasses diseases capable of afflicting virtually any part of the human body. A key aspect of cancer involves the accelerated generation of abnormal cells that proliferate beyond their usual confines. These cells can subsequently infiltrate neighboring body regions and disseminate to distant organs, a phenomenon known as metastasis. It is primarily the extensive metastatic spread of cancer that constitutes the principal underlying cause of mortality associated with cancer [2].

Figure 1.1 illustrates the incidence of new cases for the most prevalent cancer types in 2022 and their corresponding mortality rates. Leading the list in terms of mortality are lung, colorectal, and liver tumors. However, due to advancements in diagnostic techniques and more efficient treatment modalities, mortality rates have consistently decreased since the early '90s for most common cancer types, including lung, colorectal, breast, and prostate cancers [3].

In contemporary oncology, the standard treatment options include surgery, radiotherapy, and chemotherapy. These treatment modalities can be delivered

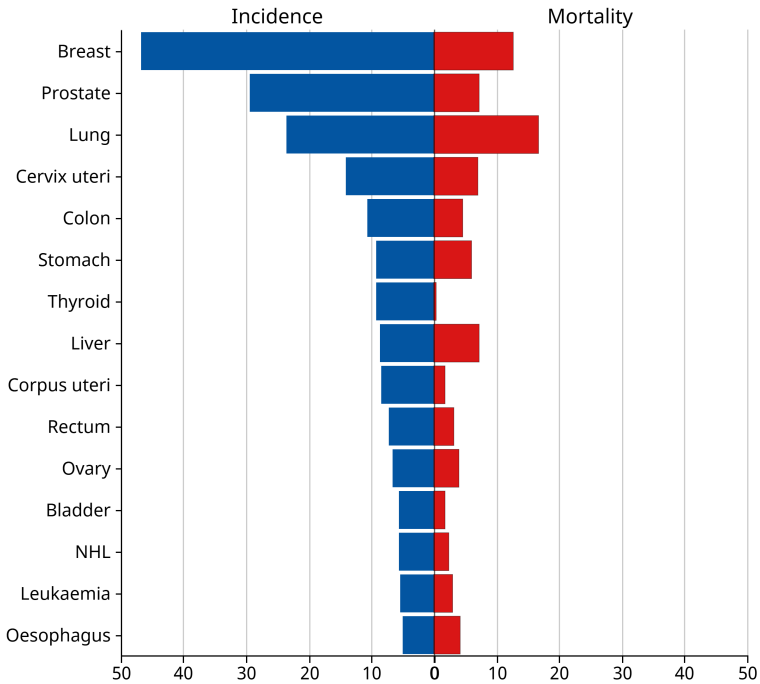

Figure 1.1: Global incidence and mortality of the 15 most common cancer types worldwide for both sexes in 2022; Data are per 100 000. Data retrieved from [1].

as individual therapies or combined. More recent modalities include hormone therapy, anti-angiogenic treatments, stem cell therapies, and immunotherapy [4].

Surgery is often the first choice for cancer treatment, but it is common to add other therapies to enhance the probability of tumor control. Radiotherapy (RT), involving the targeted delivery of ionizing radiation to the tumor, is highly effective but adds various site-specific adverse effects and systemic reactions. Chemotherapy, which employs one or more anti-cancer drugs, exhibits varying efficacy depending on the cancer type and stage. It leads to systemic reactions due to the circulation of the chemotherapeutic drugs.

Hyperthermia therapy (HT) is acknowledged as a powerful adjunct to established cancer treatment techniques, significantly enhancing the effectiveness of both RT and chemotherapy [5], [6]. HT is defined by a local temperature elevation within 40-44 °C, targeting cancerous tissue for one hour.

The potential of HT as a biological sensitizer has been extensively validated in many clinical trials when added to RT and/or chemotherapy [7]–[13]. Hyperthermia has demonstrated enhanced local tumor control, improved progression-free survival, and overall survival for various cancer types, including breast [7], [14], rectum [15], cervix [16], [17], esophagus [18], head and neck [19], sarcoma [20], and melanoma [21].

While numerous positive clinical trials support the efficacy of hyperthermia in treatment, two specific studies ([21], [22]) demonstrated that inadequate heating administration during treatment could result in no benefit. Furthermore, several studies have found a direct and positive correlation between the administered thermal dose and clinical outcomes [23]–[29], where thermal dose is a clinical measure that combines the achieved temperature in tissue and heating duration.

Bakker et al. [25] investigated 2,330 patients undergoing combined RT and HT for recurrent breast cancer. This study revealed that, on average, patients receiving a high thermal dose achieved a 34% higher complete response rate than those receiving a low thermal dose, without an increase in treatment-related toxicity. Similar results have been shown for cervix carcinomas by Kroesen et al. [28]. Valverde et al. [29] demonstrated that the therapeutic effect of hyperthermia follows a continuous thermal dose–response relationship, where progressively higher and more uniformly delivered thermal doses correlate with improved clinical outcomes.

Suboptimal heat delivery in hyperthermia treatments is frequently caused by anatomical constraints, such as the depth, vascularity, and location of the tumor, which can substantially limit the achievable temperatures. Hollow, non-solid organs, such as the bladder, pose additional challenges, as changes in filling state and motion alter their geometry and make uniform heating more difficult [30]. These challenges can often be addressed by selecting the most appropriate heating technology for the clinical scenario and through careful treatment planning.

Technical limitations also contribute significantly to inadequate tumor heating. These include inefficiencies in HT devices that fail to deliver the required thermal dose, as well as insufficient treatment monitoring and control. To mitigate these issues, quality assurance (QA) guidelines are essential. They provide standardized and robust protocols that support: (a) systematic management of the treatment process from the planning phase to results documentation, (b) comprehensive characterization of the heating capacity of the applicators, and (c) assurance of adequate safety measures for both patients and healthcare personnel. The most recent version of QA guidelines for clinical HT include superficial [31], [32], interstitial [33], and deep [34] applications.

Despite the existence of QA guidelines, their adoption in clinical settings has remained limited, as their translation into routine workflows is poorly documented, and only a few institutions have evaluated their heating systems using standardized temperature and dosimetry parameters. This limited adoption is largely due to insufficient technical expertise, the absence of practical implementation tools, including suitable tissue-mimicking materials, difficulties in achieving reliable and controlled assessments, and restricted opportunities for experimental verification.

Focus of this thesis is to support the clinical implementation of existing QA guidelines while contributing to the development of future recommendations. This is achieved through the introduction of improved phantom materials, i.e., materials designed to mimic the properties of interest of a particular tissue (or a combination of tissues), that enable systematic evaluation of HT equipment, together with demonstrations of both the practical use and the limitations of current QA procedures. In parallel, the thesis extends beyond technical validation to incorporate the regulatory perspective, integrating key principles of the European Medical Device Regulation (MDR) to establish a unified framework for the development, verification, and safe clinical deployment of

HT systems.

The thesis is structured as follows. Chapter 2 provides an overview of HT, addressing its biological effects and treatment delivery modalities, and highlights the inherent risks of HT in comparison with radiotherapy (RT). Chapter 3 examines the QA aspects of HT, outlining the fundamental principles for designing phantoms used in QA procedures. Chapter 4 demonstrates the practical implementation of QA guidelines for both superficial and deep HT, serving as a guide for these processes. Chapter 5 presents the development of a regulatory framework for HT systems under the European MDR, linking QA procedures with regulatory requirements to support device development, verification, and clinical implementation. Chapter 6 presents a concise summary of the included research papers. Finally, Chapter 7 provides concluding remarks and discusses perspectives for future research.

CHAPTER 2

Hyperthermia Principles

Electromagnetic (EM) radiation manifests as energy travelling through a medium in the form of waves or energized particles. The EM spectrum includes a wide range of EM frequencies with characteristic behaviours within certain ranges. Progressing by smaller wavelength, this spectrum includes radio waves, microwaves, infrared radiation, visible light, ultraviolet radiation, X-rays, and gamma rays. The energy conveyed by an EM wave exhibits an inverse relationship with its wavelength. Depending on the energy carried by the wave, one of the fundamental classifications is based on its ability to ionize atoms and molecules. We can then distinguish between ionizing and non-ionizing radiation, which have various applications in the medical field.

2.1 Applications of EM fields in oncology

Radiotherapy (RT) is a well-established example of the clinical use of EM fields, in which ionizing radiation induces DNA damage in cancerous tissues for curative or palliative purposes. Radiation therapy is a pivotal cancer treatment modality used in approximately 52% [35] of oncological cases. Because of the potential risk to healthy tissues surrounding the target volume, the

central objective of radiotherapy is to maximize the dose delivered to the tumour while minimizing the exposure of adjacent normal structures. This balance is achieved through advanced treatment planning techniques that rely on high-resolution imaging, such as magnetic resonance (MR) and computed tomography (CT), both themselves important medical applications of EM fields. Furthermore, fractionation strategies are employed to allow healthy tissues time to repair between treatment sessions.

Thermal therapies are not as widely used as radiotherapy, but they represent an important class of medical treatments based on non-ionizing radiation. The term thermal therapies encompasses a range of procedures that achieve therapeutic effects by transferring heat into or out of body tissues [36]. Among these, EM-based thermal therapies exploit the ability of electromagnetic waves to deposit energy in tissues through dielectric loss mechanisms. These elevated-temperature techniques are applied to treat a variety of diseases, including cancer, and are typically classified according to the temperature achieved in the target tissue: hyperthermia therapy (39–44 °C) and thermal ablation (> 47–50 °C) [37].

Thermal ablation consists of the destruction of tissue by applying heat at high temperatures (> 47–50 °C) for at least 10 minutes [38], [39]. This leads to irreversible effects such as protein denaturation, coagulation, necrosis, and apoptosis, with consequent complete cellular death. Energy is commonly administered through applicators (e.g., RF/MW antennas or laser fibers) inserted directly into the target organ [40], [41].

Hyperthermia therapy (HT), on the other hand, employs moderate temperature elevations, typically heating the tumour to 40–44 °C for around 60 minutes [37]. Both hyperthermic and ablative temperature ranges trigger a wide spectrum of biological effects, which are further discussed in Section 2.3.

These clinical applications, which rely on both ionizing and non-ionizing forms of electromagnetic energy, motivate a more detailed examination of how different types of radiation interact with biological tissues.

2.2 Interaction of ionizing and non-ionizing radiation with tissues

Radio waves and microwaves, generally considered harmless, are located on the lower energy radiation spectrum. These are labeled as non-ionizing radiation,

as their energy levels are insufficient to initiate the ionization process within the medium they traverse, precluding the emission of electrons from atoms. The non-ionizing radiation includes wavelengths longer than 100 nm [42].

Ionizing radiation is characterized by its short wavelengths and high energy levels. The minimum frequency required for radiation to be ionizing corresponds to the photon energy needed to ionize atoms or molecules—typically around 10 to 13.6 electronvolts (eV), which is the ionization energy of hydrogen. This energy range corresponds to wavelengths shorter than 100 nanometers, placing it in the extreme ultraviolet (EUV) region (wavelengths < 91 nm) and extending into the X-ray and gamma-ray parts of the electromagnetic spectrum.

Upon interaction with tissues, ionizing radiation transfers a specific amount of energy to the tissue. A straightforward method for quantifying the radiation dosage to a particular tissue volume is through the fundamental dose, denoted as D, and defined as follows:

$$D = \frac{d\bar{\epsilon}}{dm} \tag{2.1}$$

where $d\bar{\epsilon}$ represents the average amount of energy delivered to a given mass dm by the ionizing radiation. The absorbed dose is measured in joules per kilogram ($J \cdot kg^{-1}$), typically described as gray (Gy).

One of the main effects of ionizing radiation when interacting with biological tissue is to induce DNA damage. Ionizing radiation has a biological impact on DNA molecules through direct and indirect mechanisms [43]. In the direct effect, ionizing radiation directly damages the DNA molecule, disrupting its molecular structure. Such structural alterations result in cellular damage or even cell death. In this context, DNA damage typically manifests as single or double-strand breaks [44]. In the indirect mechanism, radiation interacts with tissue water molecules, which release free radicals [43]. Free radicals are highly reactive because of their unpaired electrons, and subsequently react with DNA molecules, inducing molecular structural damage.

Non-ionizing radiation is characterized by lower frequencies and photon energies, spanning a wide range from below 100 kHz (low-frequency radiofrequency, RF) up to approximately 750–940 THz (UV-A). This spectrum includes microwaves (MW), typically defined between 300 MHz and 300 GHz. At frequencies above approximately 30 MHz, dielectric losses become significant in biological tissues, particularly in those with high water content, such

as muscle. This heating effect is primarily due to the dipolar relaxation of water molecules, which attempt to align with the oscillating electric field but are unable to do so instantaneously. The resulting molecular inertia leads to internal friction and energy dissipation in the form of heat [37]. For instance, as reported by Gabriel et al.[45], the dielectric loss factor (ε'') of muscle tissue increases from approximately 2 at 10 MHz to around 50 at 100 MHz, indicating a substantial rise in energy absorption capacity with frequency. In contrast, at lower frequencies (below ∼30 MHz), ionic conduction is the dominant heating mechanism. In this regime, free ions in solution move in response to the applied electric field, generating heat through resistive (Joule) losses.

The energy absorbed in the human body due to exposure from RF/MW fields is quantified in terms of the Specific Absorption Ratio (SAR), derivable from the root mean square (RMS) electric field $\mathbf{E}$ as:

$$SAR = \frac{\sigma|\mathbf{E}|^2}{\rho} d\mathbf{r} \tag{2.2}$$

where V (m^3) represents the volume of tissue considered, σ (S/m) the tissue conductivity and ρ (kg/m^3) its density.

The energy absorbed in tissue is then converted to heat, thus inducing a temperature increase. For living biological tissues, a critical parameter that influences this temperature increase is blood perfusion, which acts as a convective heat sink. A widely recognized model that incorporates the influence of blood perfusion is the Pennes' bio-heat equation [46]:

$$c\rho\frac{\partial T}{\partial t} = \nabla \cdot (k\nabla T) - c_b w_b (T - T_b) + P \tag{2.3}$$

where k ($W/m/K$) is the tissue thermal conductivity, c ($J/kg/K$) is its specific heat capacity, T ($^\circ C$) is the temperature, P (W/m^3) is the power density; c_b, w_b ($kg/s/m^3$) are the blood heat capacity and perfusion rate, respectively; and and T_b is arterial temperature

2.3 Biological effects of heat

The application of heat within the HT temperature range triggers a wide array of direct and indirect effects that enhance the sensitivity of tumor cells to other firmly established treatments, such as chemotherapy and radiotherapy [47],

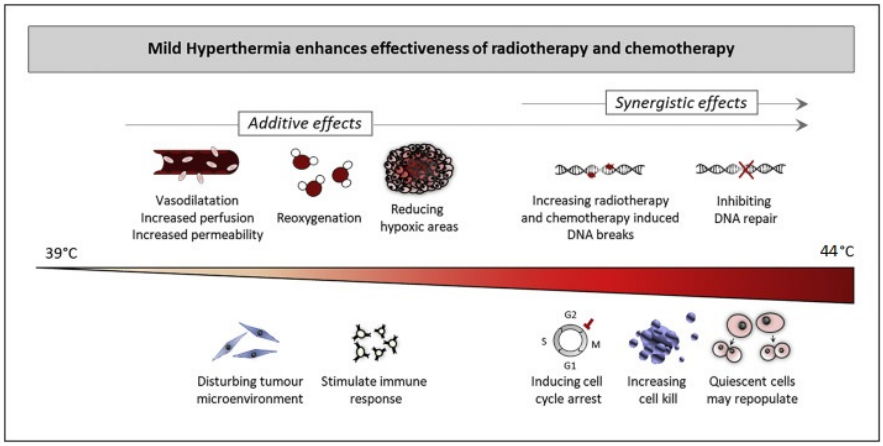

Figure 2.1: Summary of the synergetic and additive effects of hyperthermia, depending on the temperature. Adapted from [50]. Hyperthermia, up to 44 °C, induces vasodilation, enhancing blood perfusion for deeper penetration of chemotherapeutic agents. This increased permeability boosts oxygenation, intensifies radiation-induced DNA breaks, and reduces tumour hypoxic areas, altering the micro-environment and stimulating immune responses. Additionally, mild hyperthermia amplifies residual DNA breaks, promoting cell cycle arrest and making cells more susceptible to radiotherapy and hyperthermia, especially if temperatures exceed 41 °C, as it inhibits DNA repair.

[48]. The biological mechanisms induced by HT are discussed comprehensively in [49], [50].

A fundamental characteristic of HT is that its biological impact depends strongly on both the temperature achieved and the duration of heating. The dependency of HT effects on the temperature is summarized in Figure 2.1. In vitro studies have shown that prolonged exposure to elevated temperatures increases cell death and suppresses DNA damage repair pathways [51].

Temperatures above 39 °C trigger a physiological response characterised by increased perfusion and enhanced vascular permeability, leading to significant changes in the tumour micro-environment. These alterations improve oxygenation and pH levels, thereby increasing the tumour's sensitivity to radiation-induced damage [52]. At the cellular level, mild hyperthermia increases membrane fluidity, which enhances the uptake of chemotherapeutic

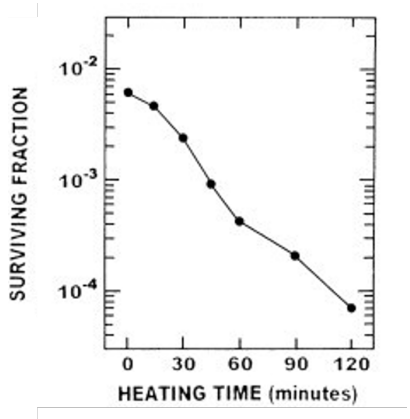

Figure 2.2: Response of HA-1 cells to irradiation with 12 Gy and then immediately heated at 43 °C for different times. Reprinted from [5]

agents [53]. Improved perfusion at these temperatures also facilitates the recruitment of immune cells to the tumour site [54], supporting the initiation of hyperthermia-induced immune responses. Evidence indicates that this immune activation is particularly effective in the 40–41 °C range [5], [55]. Localised heating has additionally been shown to enhance cytotoxic T-cell activation and can induce a systemic immune response targeting tumour cells distant from the heated region, a phenomenon often described as an abscopal-like effect [56].

In the 41–43 °C range, direct molecular effects of hyperthermia become dominant. Elevated temperatures inhibit key DNA repair pathways, reducing the activity of proteins involved in repairing radiation-induced DNA damage [57]. This includes the suppression of homologous recombination, a major mechanism for repairing double-strand breaks [58]. Inhibition of these pathways leads to the accumulation of residual DNA breaks, thereby increasing treatment efficacy. Studies have shown that prolonged heating within this temperature window markedly increases cytotoxicity [59], underscoring the importance of both temperature and exposure duration.

The interaction between heating duration and biological effect is illustrated in Figure 2.2, where the survival fraction of HA-1 cells is shown following 12 Gy irradiation and subsequent heating at 43 °C for different time intervals.

Increasing heating duration results in progressively reduced cell survival, confirming the strong time dependence of HT-induced sensitisation. However, extended exposure also activates the heat-shock response—a protective mechanism characterised by the rapid synthesis of heat-shock proteins (HSPs) [60]. This response leads to thermotolerance, a temporary reduction in cellular sensitivity to subsequent hyperthermia treatments lasting 48–72 hours. Consequently, clinical hyperthermia sessions are typically limited to about 1.5 hours and scheduled no more than twice per week, ensuring therapeutic benefit while minimising the onset of thermotolerance.

2.4 Thermal dose

Thermal therapy treatments can be quantified in terms of thermal isoeffective dose, or simply thermal dose, which represents the combined impact of temperature and treatment duration expressed in terms of an equivalent time at the reference temperature 43 °C to reflect the effect of the temperature to direct cell death [61].

A standard definition for thermal dose is the cumulative equivalent minutes at 43 °C (CEM43) [62], representing the effect of the entire history of heat exposure on cell death. This definition allows the comparison of HT treatments with different temperatures and heating durations. CEM43 does not take into account the radio- or chemo-sensitizing effects of heat, but it is still the most widely used metric for thermal therapy treatments, acting as a de facto standard. Following this definition, the equivalent thermal dose can be expressed as:

$$CEM43 = \sum_{t=0}^{t=t_{total}} R^{(43^{\circ}C-T)}\Delta t \tag{2.4}$$

where t_{total} is the total treatment time, Δt (min) is the take between two consecutive temperature measurements, while T(°C) is the average temperature during the interval Δt. R assumes a value of 0.25 for T $<$ 43 °C and 0.5 for T $\geq$ 43 °C [63], and it is based on the biphasic Arrhenius plots.

The CEM43 model, however, has limitations due to its assumption that different tissues share the same heat sensitivity and its inability to account for the radiosensitization capability of HT [64]. In response to these limitations,

various variants of CEM43 have been introduced. These variants incorporate temperature indices, such as T90, T50, or T10, into the CEM43 definition, where Tx is the tumour temperature exceeded by x% of the measured temperature points. This adaptation aims to address the heterogeneous temperature distribution observed in vivo. The resulting parameters are referred to as CEM43T90 [65].

While CEM43 and its variants capture the dominant biological effect at high temperatures, in most clinical studies, it is often noted that the actual tumour temperatures recorded are lower than the intended 43°C. Consequently, alternative parameters have been proposed over the years. Clinical outcomes are typically reported in terms of maximum(T_{max}), minimum (T_{min}), and average (T_{avg}) temperatures and more often T90, T50, or T10. These parameters are also recommended in the most recent quality assurance protocols for superficial HT [31].

The TRISE parameter is proposed in [27] as an alternative to these parameters. TRISE integrates both temperature and heating duration. However, instead of converting the recorded temperatures into equivalent minutes at a reference temperature, the T50 increase above 37 °C throughout the treatment is directly multiplied by the treatment duration. The result is then normalized to the total scheduled treatment time (set to 450 min):

$$TRISE = \frac{\sum_1^n (T_{50} - 37°C) \cdot dt}{450} \tag{2.5}$$

where dt is the treatment duration and n is the number of treatments.

The area under the curve above 39 °C (AUC $\geq$ 39 °C) for transient temperature was introduced by Datta et al. [66] as a straightforward parameter that integrates both time and temperature. This measure captures the multifactorial nature of HT effects across the entire relevant temperature range and is defined as follows:

$$AUC \geq 39°C = \sum_{n=1}^{N} \Big(\frac{T_{n-1} + T_n}{2} - 38.9 \Big) (t_n - t_{n-1}) \tag{2.6}$$

where T_n denotes the temperature at the time instant t_n.

Although several parameters have been proposed, a consensus on a temperature or thermal-dose metric capable of reliably characterising the dose–effect relationship in clinical HT has yet to be established [67]. This lack of agree-

ment is largely attributable to limitations in thermometry, such as the small number of probes, restricted placement relative to the tumour, and insufficient temporal sampling, as well as inconsistencies in how temperature metrics are defined and reported. These factors hinder a robust interpretation of tumour temperature coverage and complicate the assessment of dose–effect relationships. Nonetheless, the currently used temperature metrics remain essential for promoting standardisation and enabling comparison across clinical studies.

In contrast to RT, delivering a prescribed thermal dose in HT remains a challenge. Biological heterogeneity, such as variations in tissue composition, perfusion, and vascular dynamics, leads to highly non-uniform heating within the target region. In addition, the effective performance of heating systems depends on correct operation, calibration, and configuration, all of which influence the temperatures that can be safely and consistently achieved in deep or heterogeneous tissues. Consequently, rigorous assessment of device heating performance is essential to ensure that an adequate and therapeutically meaningful dose distribution can be delivered. Quality assurance protocols provide structured and reproducible procedures to verify system function and performance, and are therefore critical to maximising therapeutic efficacy and ensuring safe clinical application.

Strong clinical evidence highlights an association between suboptimal heating quality and unfavourable clinical outcomes. This can be attributed to both the heating inability of HT equipment and inadequate temperature monitoring. The findings presented by Perez et al. [22] do not indicate significant improvements when using RT alone compared to RT+HT in the treatment of large superficial lesions (> 3 cm). The leading cause for this negative result is attributed to the absence of stringent guidelines for patient and tumour selection in HT clinical trials as well as the absence of rigorous QA protocols for evaluating device performance. On the other hand, evidence has emerged over the years, pointing to a positive correlation between temperature, the thermal dose delivered within the target, and clinical outcomes [23]–[27], [29], [68]. Higher thermal dose is associated with increased local tumour control and higher complete response rates. A recent example is provided by Bakker et al. [68], who reported that recurrent breast cancer patients who received a higher thermal dose (specifically CEM43T50 ≥ 7.5 min in their best session) achieved significantly improved locoregional control (see Figure 2.3). These findings underscore that achieving adequate temperature coverage and suf-

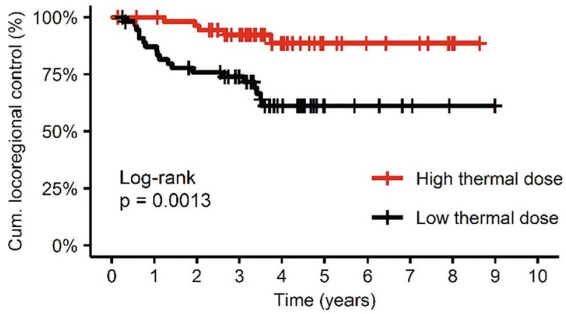

Figure 2.3: Kaplan–Meier curves illustrating locoregional control stratified by thermal-dose group for a 112 patients with resected locoregional recurrent breast cancer treated with postoperative re-irradiation plus HT: patients treated with high thermal dose (best CEM43T50 $\geq$ 7.2 min) show substantially better 3-year locoregional control ($\approx$ 92 %) compared to low-dose patients ($\approx$74 %) (p = 0.008) . Reprinted from [68]

ficient dwell time (i.e., sustained therapeutic heating) is essential; it is not merely the application of hyperthermia, but the quality of heating that determines clinical benefit.

2.5 Adverse effects associated with RT and HT

RT is a complex treatment modality associated with substantial risks. The estimated incidence of errors in radiotherapy is approximately 0.15% [69], with around 40% of these incidents resulting in patient harm and about 1% leading to fatal outcomes. In addition to the risk of accidental misadministration, RT itself produces a broad spectrum of adverse effects that vary with the treatment site. Beyond inducing direct DNA damage, ionizing radiation activates multiple cellular signalling pathways, triggering pro-inflammatory and pro-fibrotic cytokine expression, coagulation cascades, and vascular injury [70]. These biological responses contribute to the development of oedema, inflammation, skin erythema, elevated intracranial pressure in central nervous system treatments, and pulmonary fibrosis in thoracic irradiation [71]. For abdominal and pelvic treatments, gastrointestinal toxicity is common, manifesting as anorexia, nausea, vomiting, abdominal cramps, and diarrhoea. Irra-

diation of the pelvis may also impair bladder function and lead to conditions such as cervicitis and vaginitis in women [71].

To mitigate these risks, systematic QA programs are fully embedded in routine RT practice. These programs ensure accurate dose delivery, reduce the likelihood of errors, and help limit severe or irreversible side effects. A detailed overview of the QA and safety measures used in RT is provided in the following chapter.

HT, in contrast, uses non-ionizing electromagnetic radiation, typically in the RF/MW range, to raise tissue temperature for therapeutic benefit. Although significantly less hazardous than ionizing radiation, HT still requires careful energy delivery to avoid potential harm to both patients and medical staff. Similar to RT, the risks associated with HT can be categorised into direct and indirect effects. Direct effects arise from the absorption of electromagnetic energy, resulting in tissue heating—the therapeutic objective—but inadvertently also producing local hotspots, superficial burns, or circulatory disturbances when excessive cooling is applied [72].

Indirect potential risks rise from the interaction between electromagnetic fields and conductive materials. Electrical currents induced in metallic objects may cause burns at points of contact, and the EM fields generated during HT can interfere with metallic medical implants and other implanted devices such as pacemakers, making them contraindications for many EM-based HT systems [73]. Where feasible, treatment planning is used to steer energy away from such devices.

It is the responsibility of the clinical staff to ensure that the maximum and effective thermal dose is delivered while maintaining patient safety throughout the procedure to prevent any direct or indirect adverse effects. Effective audible and visual communication with the patient is essential to obtain immediate feedback in case of discomfort and to enable prompt intervention when needed.

To ensure staff safety, HT facilities must implement comprehensive electromagnetic-field (EMF) protection measures and verify compliance with national exposure limits for non-ionizing radiation within the HT frequency range. Standards such as IEEE C95.1-2019 [74] and the 2020 ICNIRP guidelines [75] specify maximum permissible occupational exposure levels of approximately $10\,\mathrm{W/m^2}$ in this frequency band. Proper shielding of the treatment room minimises electromagnetic leakage, protecting both equipment and staff; however, staff

exposure is typically negligible due to the very low SAR levels present outside the applicator field. Patients are exempt from occupational exposure limits because the therapeutic benefits of HT outweigh the minimal risks associated with controlled EMF exposure.

Finally, well-designed QA procedures are essential not only for ensuring patient and operator safety but also for achieving uniform heating and consistent treatment performance across clinical sessions.

2.6 Hyperthermia Delivery

HT systems architecture

As illustrated in Figure 2.4, a generic HT system consists of four fundamental components:

Signal generation and amplification unit: This block generates the therapeutic signal at the desired operating frequency and amplifies it to the required power level. In phased-array systems—where multiple antenna elements are arranged around the patient—each channel can be individually controlled in amplitude and phase. Phase shifters are essential for electronically steering the focal point toward the target region.

Applicator: The applicator delivers energy to the patient and varies according to the HT modality and anatomical site. It may consist of single or arrayed antennas, infrared emitters, or capacitive electrodes. In radiative HT, external antennas require a coupling medium to interface with the body; deionized water is typically used to minimise field perturbations and is contained within a water bolus made of skin-compatible plastic. The bolus not only ensures proper electromagnetic coupling but also provides controlled skin cooling through an integrated circulation system, reducing the risk of superficial burns. Applicators can also be placed internally or intracavitarily, depending on the clinical scenario.

Thermometry: Thermometry is essential for measuring the temperature achieved in or near the target volume. Available techniques depend on the application and include invasive probes placed within catheters in body cavities or directly in tissue, as well as non-invasive surface sensors for superficial treatments. Some centres also use invasive catheters for superficial lesions

to monitor subsurface temperatures more accurately. Temperature probes may operate in a static modality, where the probe remains fixed at a specific position within the catheter (e.g. multisensor fiber-optic probes), or in a dynamic modality. In the second case, a thermal mapping system is usually employed. In this setup, the probes are mechanically pulled by a device, known as *mapper*, which moves them in fixed steps over a user-defined distance to record the temperature distribution along the catheter path. Non invasive thermometry modalities are available,. although not widely deployed clinically. The most used is magnetic resonance (MR) thermometry, which provides a non-invasive alternative capable of delivering quasi–real-time 3D temperature maps, even if this technique is highly sensitive to motion, which can cause temperature errors of several degrees.

Control and treatment planning unit: This unit regulates the power delivered to the applicator and, in phased-array systems, adjusts the phase distribution according to the treatment plan. Modifications to antenna settings can be made either manually or semi-automatically during treatment, guided by feedback from thermometry or from measurements of amplitude and phase at the applicator ports. At present, treatments still rely heavily on manual intervention, and fully automated adaptive control systems have not yet been implemented in routine clinical practice.

HT modalities

Different technologies are available to achieve the therapeutic temperature range HT requires [76]: 40-44 °C for 1 hour. Depending on the tumour location and size, the most common HT applications are superficial HT, deep HT, interstitial HT, and intracavitary HT. When heating is applied to the entire body rather than a specific target volume, the technique is referred to as whole-body hyperthermia. These delivery modalities are illustrated in Figure 2.5.

Hyperthermia treatments can be delivered using a range of technologies. Among these, EM-based approaches, including capacitive, radiative, and infrared systems, are the most clinically used, largely due to their versatility and ability to target diverse anatomical regions. Non-EM modalities, such as high-intensity focused ultrasound (HIFU) and perfusion-based hyperthermia, also exist and provide additional options for achieving therapeutic temperatures.

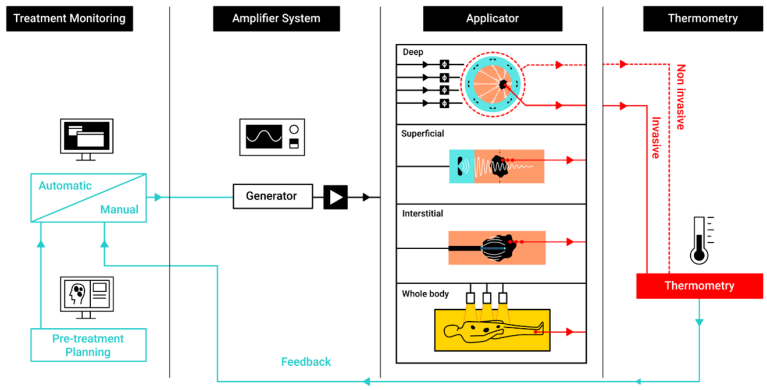

Figure 2.4: EM HT system decomposed in its main four subsystems. Different applicators are considered depending on the treatment technique.

Superficial HT Superficial HT is intended for the treatment of lesions located up to approximately 4 cm beneath the skin surface. Typical indications include lymph node metastases from head and neck cancer, breast cancer, chest wall recurrences, and melanoma lesions [77]. Treatment is delivered using external applicators—such as microwave antennas in single or array configurations, capacitive electrodes, or infrared lamps.

Superficial HT systems typically operate in the 400 MHz–1 GHz frequency range, as these frequencies allow preferential energy deposition within the first few centimetres of tissue [77]. Common clinical implementations include waveguide-based applicators, such as the 434 MHz Lucite Cone Applicator used at Erasmus MC in Rotterdam [78], and the 915 MHz BSD-500 system (Pyrexar Medical, Salt Lake City, UT, USA). Other designs use microstrip antennas, such as the Conformal Microwave Array (CMA) [79], and commercially available systems like the ALBA ON 4000 (ALBA Hyperthermia, Rome, Italy), which operates at 434 MHz with antennas of fixed curvature. In all these systems, multiple antenna elements may be combined to enlarge the treated area.

Capacitive systems use metal electrodes operating at frequencies of 8, 13.56, or 27.12 MHz [76]. Localized heat delivery is achieved using electrodes of different dimensions, where the RF fields concentrate near the smaller elec-

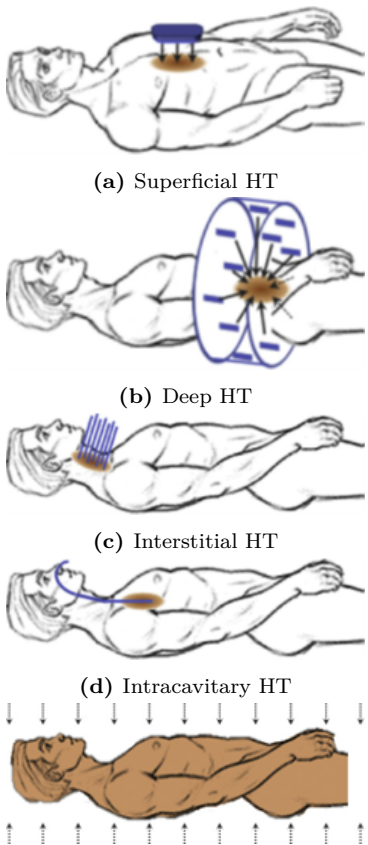

(a) Superficial HT

(b) Deep HT

(c) Interstitial HT

(d) Intracavitary HT

(e) Whole-body HT

Figure 2.5: Graphical representation of the most common HT application modalities. Reprinted from [77]

trode. However, this technique may result in excessive fatty tissue heating due to the orientation of the main electric field component perpendicular to the fat–muscle interface. [80]–[82]. This is not the case for the radiative applicators, for which the field components are parallel to the interfaces between superficial fat and muscle. The interface conditions, as per Maxwell's equations, specify that the tangential E-field remains continuous while the normal E-field component experiences a discontinuity proportionate to the dielectric properties of the two distinct tissues. This results in a considerably increased electric field within the fat tissue when utilizing capacitive systems.

Infrared HT uses infrared lamps operating above 300 GHz [76]. The penetration depth of the infrared radiation is usually less than 1 cm. Still, by using customized filters, this technology can treat lesions infiltrating up to 1.5 cm below the skin surface [83]. For deeper targets, MW and RF systems are preferred.

Deep HT Deep HT targets tumours deeper than 4 cm from the skin surface. The heat is administered externally. Radiative RF and MW devices are the most commonly used, but capacitive technology is gaining attraction due to the lower acquisition cost and simpler system architecture. Radiative deep HT has demonstrated strong clinical performance, particularly for tumours in the pelvic and abdominal regions, such as cervical, bladder, and rectal cancers, as well as sarcomas and paediatric malignancies, with several studies reporting excellent treatment outcomes [12], [15], [84]–[86].

In radiative deep HT, treatment is often delivered using phased-array systems consisting of multiple antennas organized in one or more rings around the body. These systems allow power steering by adjusting the phase and amplitude settings of each antenna or of sets of antennas. A focus in the target volume is achieved by optimizing the phase and amplitude settings to obtain constructive interference within the tumour [87], [88]. The typical frequency range used in radiative deep HT is 70-150 MHz, enabling a heating focus with a diameter of 10–15 cm [76]. Commercial solutions include the four-channel BSD-2000 system (Pyrexar Medical, Salt Lake City, UT, USA), available with various applicators tailored to specific anatomical sites, as well as the Alba 4D system (Med-Logix SRL, Rome, Italy), which employs four waveguides. Modern experimental systems aim to achieve smaller focal spots by using higher frequencies and broadband antenna designs [89], [90].

Capacitive devices typically feature two electrodes with a diameter equal to or greater than 25 cm. However, this technique exhibits notable limitations. The uniform size of the electrodes restricts the ability to adjust the focus, thereby limiting control of the emitted power. Additionally, a substantial portion of the power is absorbed by the superficial fat layer, limiting the penetration to the desired depth. Moreover, the only way to control the shape and location of the focus is through the placement and dimensions of the electrodes used.

Interstitial and intracavitary HT In interstitial HT, needle-shaped antennas are percutaneously inserted into the target tissue, typically operating between 500 MHz and 1.3 GHz [91]. These antenna elements have a typical active length of 4-10 cm and a diameter of 1-2 mm [36]. Various antennas have been explored to achieve interstitial heating, including the monopole, dipole, slot, and helical coil microwave antennas [76]. Interstitial MW hyperthermia has been shown to be effective in heating tumours and achieving local control in randomized trials, mainly when used in combination with brachytherapy [92], [93].

In intracavitary HT, the antenna elements are inserted into the body via natural cavities and orifices, such as the vagina, rectum, oesophagus, urethra, or bladder. The heating is primarily focused on the cavity and its immediate surroundings, reaching depths of up to 1 cm from the lumen. The applicators used in intracavitary HT are typically similar to those used in interstitial HT and have comparable active lengths but diameters up to 30 mm [77].

Whole body HT Whole body HT uses radiant heat and infrared lamps to induce a systemic body temperature increase for a prolonged time interval. This can be achieved within the ranges of 39–40 °C for 6 hours (referred to as fever-range whole body HT) or 41–42 °C for 60 minutes (considered extreme whole body HT) [94], [95]. This approach is beneficial for treating distant metastases and non-solid malignancies.

CHAPTER 3

Quality Assurance Protocols

The term Quality Assurance (QA), as defined by the International Standard Organization (ISO), is "all those planned or systematic actions necessary to provide adequate confidence that a product or service will satisfy given requirements for quality" [96]. In the medical context, this concept translates into efforts aimed at monitoring the quality of care provided to individuals or groups of patients, enabling the identification of potential deficiencies and facilitating corrective actions. A prime illustration of this can be found in radiation oncology, where QA programs form an integral part of radiation therapy practice [97], due to the associated biological effects of ionizing radiation. These programs play a pivotal role in minimizing the probability of accidents and errors enhancing the safety and comfort of patients and healthcare workers.

While not as firmly established as in RT, QA procedures for HT have been available since its early days, covering both deep and superficial treatments [22], [98]. Over the years, these guidelines have been revised reflecting the increased knowledge and technological development [99], [100] until the most recent versions for deep [34], [101], superficial [32], and interstitial HT [33] QA protocols. These guidelines aim to ensure a uniform QA and treatment

control level across different institutions.

Furthermore, the development of these guidelines addresses the need to harmonize HT practices with RT quality level, since the two modalities are frequently delivered in combination within the same clinical workflow.

This chapter begins with a review of the most recent QA procedures in both radiotherapy and hyperthermia. The focus then shifts to hyperthermia, with the aim of identifying its clinical and technical requirements and examining the strategies developed to meet them, including the design of tissue-equivalent materials for the practical implementation of clinical guidelines.

3.1 QA guidelines in RT

QA programs are solidly settled and well integrated into modern radiation oncology, providing one of the most indicative examples of QA assuming a primary role in clinical practice. The need for rigorous QA procedures in RT arises from the inherent risks associated with ionizing radiation and the demand for highly precise dose control. Normal tissue tolerance thresholds are narrow, and tumour response is strongly correlated with the accuracy of the delivered dose [102]. Moreover, the technology used in RT devices is complex [97].

An initial effort to achieve these goals can be traced back to the late 70s, with the publication of the International Commission on Radiation Units and Measurements Report, which prescribed the requirement of dose delivery precision within 5% [103]. Since then, QA protocols have evolved following the development of technology, such as integrating image-based techniques and 3D treatment planning systems.

It has been demonstrated that implementing a robust QA program in RT can impact patient survival rates in the long term [104]. The rationale for a QA program in radiotherapy is based on four fundamental aspects [105]:

1. Reducing errors in treatment planning and dose delivery to enhance remission rates and minimize the risk of complications.

2. Ensuring consistent dosimetry and treatment control across various institutions, facilitating inter-institutional comparisons.

3. Optimizing the treatment's effectiveness by fully exploiting the capabilities of modern radiotherapy technology.

4. Ensuring uniform treatment quality in developed and developing countries.

A brief overview of a general QA protocol in RT is provided in reference [106]. The main target is to meet the 5% delivery precision requirements for the prescribed dose.

In modern RT, QA includes three crucial domains of treatment: clinical, physical, and technical. This comprehensive approach ensures a thorough coverage of all aspects of a typical RT treatment program, including treatment planning, beam delivery, and treatment documentation:

Treatment planning: This is a complex process that involves collaboration among various specialties, such as radiation oncologists, dosimetrists, and medical physicists. QA guidelines play a pivotal role throughout the entire process, starting with the treatment prescription and continuing through planning and treatment verification:

- Prescription: Stringent requirements are imposed for written and certified documentation.
- Patient data acquisition: QA procedures are in place for CT and MR scans, including assessments of image quality. Patient positioning is facilitated through laser alignment.
- Contouring and target volume definition: Specific QA actions are prescribed for the treatment planning system, and a peer-review process is recommended to ensure high-quality contouring and tissue delineation.
- Specific requirements apply to the treatment planning software. Tolerance levels of 2% are set for the source isodose distribution. Periodic verifications are mandated, ranging from daily tests for I/O device functionality to annual reference QA tests.

Beam delivery: The efficacy of treatment delivery is closely linked to the functional performance of therapy equipment, which directly impacts dosimetry accuracy and the patient's received dose. QA tests are prescribed, with tolerance values and recommended frequencies varying according to their impact on the patient. Daily QA tests include laser positioning verification, while mechanical tests, such as gantry and collimator isocenter verification, are conducted monthly. Phantom dosimetry may be employed to measure absorbed dose distributions with high spatial resolution [107]. In addition,

patient positioning and setup verification are essential components of QA during beam delivery. Before each treatment fraction, the patient must be accurately aligned with the treatment isocenter to ensure that the planned dose distribution matches the intended anatomical target. Daily setup procedures typically involve the use of room lasers, immobilization devices, and image-guided radiotherapy (IGRT) systems such as kV/MV planar imaging and cone-beam CT (CBCT), following the recommendations of established QA protocols [108], [109]. These procedures significantly reduce geometric uncertainties and help ensure reproducible positioning across treatment sessions.

Treatment documentation: the recording of patient identification data, treatment planning details, and the execution of treatment is crucial. This information is documented in a patient's chart, which undergoes regular review by a multidisciplinary team during treatment and upon completion. The transfer of information is also subject to specific QA procedures, as outlined in [110].

3.2 QA guidelines in HT

Similarly to RT, QA protocols in HT are designed to ensure that heating devices consistently deliver safe and effective treatments. The focus extends beyond verifying that the system can achieve the prescribed thermal dose; it also includes a comprehensive evaluation of all factors that influence treatment quality. As in radiotherapy, QA guidelines in HT address a broad range of clinical and physical considerations, such as:

Treatment planning: The primary goal of HT treatment planning is to maximize the SAR and/or temperature coverage within the target while minimizing energy deposition in healthy tissue. In clinical practice, temperature constraints are applied to reduce the risk of thermal injury to surrounding organs. A commonly used upper limit for normal tissue is approximately 44 °C [101], while more conservative thresholds (around 42–43 °C) may be adopted for thermally sensitive structures such as bone marrow or the nervous system. However, these values should be regarded as guidance rather than strict universal standards, as thermal tolerance varies across tissues and depends on exposure duration and perfusion conditions. Thus, the compu-

tational model should match the anatomy, applicator, and clinical setup as closely as possible. Currently, no formal technical standards exist for the computational methods employed in HT treatment planning. Nonetheless, recent work has introduced structured modelling guidelines and benchmark recommendations that may serve as a basis for future standardization [111].

Treatment delivery: Accurate delivery of the prescribed thermal dose requires careful patient preparation and effective treatment monitoring. These critical aspects are addressed in the QA guidelines and can be summarized in three key components:

- Patient positioning: A high degree of positioning accuracy, within 1 cm of the modelled position during the planning phase, is required [112]. To achieve this precision, clinical staff use side lasers and markers corresponding to the applicator edges for tailoring and adjustments.
- Temperature monitoring: Multi-sensor probes and/or thermal mapping systems are required, while non-invasive temperature sensors or MR-based thermometry are valuable add-ons. At least one sensor must be related to the tumour temperature. It is crucial that these sensors exhibit minimal or no interaction with the EM field, and measures must be taken to prevent self-heating phenomena caused by the probes[67]. Thermometry equipment should meet specific requirements regarding an accuracy of ± 0.2 °C [32]. In cases where thermal mapping is used, a track length of at least 15 cm is recommended [113].
- Treatment documentation: Maintaining standardized and comprehensive treatment documentation is essential, as it is a requirement for evaluating treatment effectiveness [67]. This documentation should include patient treatment setup, HT applicators used and their settings, thermometry, and power data. Standardized temperature parameters such as T90, T50, T10, maximum and mean tumour temperatures should be recorded. Additionally, any patient complaints and acute toxicities observed during the treatment must be reported.

Requirements and characterization of equipment: An HT system must meet specific technical requirements to deliver targeted heating to the treatment volume while safeguarding surrounding tissues. Reliable control of the EM fields generated by the applicator is essential for accurate treatment delivery. In radiative HT systems, this involves maintaining frequency-

dependent accuracy in amplitude and phase control, leading to maximum acceptable focal shifts on the order of 1–2 cm, depending on the anatomical site [34]. Phase and amplitude accuracy can be verified at the amplifier level using standard RF measurement equipment, such as power meters. The physical characterization of the HT applicator is commonly performed using appropriately designed tissue-mimicking phantoms, where the heating patterns produced by the device are analysed. This component forms a central focus of the present work and will be examined in greater detail in the following sections.

Staff requirements and safety: Guidelines also address staff qualifications and safety considerations within HT facilities. The treatment team should ideally include a well-trained physician and a medical physicist. As no formal certification for hyperthermia physicists currently exists, many institutions employ engineers with backgrounds in physics or medical sciences to fulfil this role [114]. Detailed recommendations regarding the responsibilities and required competencies of HT personnel are available in [115]. For aspects related to patient safety and staff EMF protection, see Paragraph 2.5.

The existing guidelines comprehensively address the clinical aspects of QA in HT, including deep [34], superficial [32], and interstitial HT [33]. These clinical aspects will not be further elaborated upon in this work. Instead, our focus is directed towards novel techniques for evaluating the performance of HT systems.

Instrumentation and operating conditions for QA procedures

The QA verification of heating devices must be carried out under reproducible conditions. This requires the establishment of a common and defined experimental QA protocol. A shared prerequisite for all QA procedures is achieving thermal equilibrium with room temperature at the start of experiments. When water bolus is used as a coupling medium between the applicator and phantom, it is preferable that the water circulates and remains at room temperature to prevent any disruption to the heating pattern. To guarantee reproducibility, it is crucial to ensure proper and consistent positioning of the applicator relative to the phantom.

The minimum set of QA instrumentation required should allow proper monitoring of the temperature distribution and, specifically for deep HT systems,

achieving a clear focal volume. More specifically, this includes:

Standardized phantoms: A tissue-equivalent phantom is typically defined as an object designed to replicate the relevant physical properties of biological tissue. The geometry and composition of a phantom depend on the technology or applicator being evaluated, as discussed in later sections. A key distinction exists between tissue-equivalent phantoms used to analyse spatial temperature patterns and lamp phantoms, which are employed for rapid assessment of EM-field symmetry and beam-steering performance in deep HT applicators.

Temperature probes: Temperature probes used in HT treatments should undergo daily verification to ensure calibration within ± 0.2 °C. Probes that fall outside this tolerance must be recalibrated against a reference standard until the required accuracy is restored. To enhance temperature spatial resolution, two probe configurations are commonly used: multi-sensor probes and thermal-mapping probes. These contrast with stationary single-sensor probes that provide only one measurement point. In thermal mapping, probes are inserted into a catheter and translated cyclically—either mechanically or manually—to sample temperature distributions across the region of interest, including both the tumour and surrounding tissues.

IR camera: Infrared (IR) cameras are particularly relevant for QA procedures involving solid or split phantoms in superficial and interstitial HT. The IR camera must provide sufficient accuracy and thermal sensitivity to reliably visualize and quantify the 2D surface temperature distribution induced by the HT applicator.

Additional instrumentation: A more quantitative assessment of HT applicator performance can be obtained using E-field probes. These may be scanned in 3D water tanks to generate volumetric SAR maps or employed as dipole probes with high-resistance leads [116]. Measurements of antenna efficiency and power reflection can be performed using a vector network analyser (VNA), or alternatively, a power meter. A dielectric properties measurement kit and a thermal properties analyser are required for the characterization of tissue mimicking phantoms. Finally, the conductivity of the bolus water can be periodically verified with a conductometer to exclude the presence of metallic contaminants.

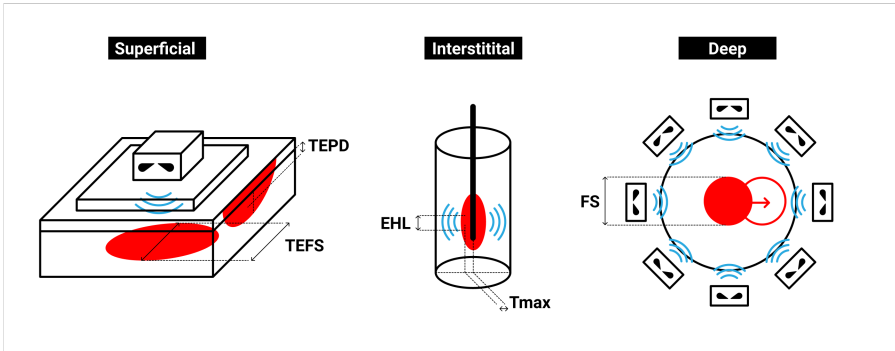

Figure 3.1: Quality metrics currently defined for the QA assessment of superficial, interstitial, and deep HT. Available from: http://www.esho.info/.

General requirements for HT equipment

Evaluating the performance of HT equipment requires clear and measurable criteria that can be reliably assessed under controlled conditions. Homogeneous tissue-mimicking phantoms are typically used for this purpose, as they enable reproducible testing of heating capabilities without the confounding effects of patient-specific variability. A required benchmark for determining whether a heating device is suitable for clinical HT applications is its ability to achieve a temperature rise (TR) of 6 °C within a defined time interval in a homogeneous phantom. This target reflects the clinical requirement of raising tissue temperature from core body temperature (∼37 °C) to the therapeutic HT range of approximately 43 °C.

The specific conditions under which the 6 °C rise must be obtained depend on the HT modality. For superficial and interstitial HT, the criterion requires reaching this temperature increase within 6 minutes at a depth of 1 cm in a muscle-equivalent phantom. The same 6-minute criterion applies to deep HT systems designed for head-and-neck or distal extremity treatments, where the temperature rise is evaluated at the phantom middle. Deep HT applicators targeting abdominal or pelvic regions are instead assessed based on achieving the 6 °C increase within 10 minutes. For interstitial HT, the temperature rise must be achieved at a distance of 0.5 cm from the applicator surface. These requirements are derived from prior studies evaluating HT system performance [117], [118].

For deep HT systems, an additional requirement is the focusing ability, referring to the capacity of the applicator to generate and steer the focal region within the intended treatment volume. This characteristic can be evaluated in terms of both energy deposition and the resulting temperature distribution, as described in later sections.

Additional HT-technique specific quality metrics can be derived from the thermal distribution generated by the applicator. These metrics are graphically summarized in Figure 3.1 and described in the following paragraphs.

Technique specific requirements

In this thesis, the primary focus is on QA protocols for superficial and deep HT; therefore, the following sections concentrate on these two modalities. Current QA guidelines for interstitial HT are available in [33].

Superficial HT Superficial HT is a technique intended to target lesions located within 4 cm from the skin surface [76]. Consequently, assessing the device's capability to provide effective heating in a volume close to the applicator is crucial. The ESHO QA guidelines for superficial HT [32] prescribe two quality indicators to quantify the applicator heating performance, complementary to the TR.

The evaluation of these parameters is carried out using tissue-equivalent phantoms, which must accurately replicate the electrical or acoustic properties, depending on the heating technology in question, as well as the thermal properties of human tissue. The muscle-mimicking phantom is divided into different solid phantom layers to facilitate the temperature reconstruction generated by the applicator, where the layer thicknesses depend on the applicator operating frequency. The uppermost 1 cm layer is a fat-mimicking phantom, while the underlying layers consist of muscle-equivalent material. Figures 3.2a and 3.2b illustrate the recommended phantom configurations for operating frequencies below 915 MHz and at or above 915 MHz, respectively.

The 2D thermal distribution at each interface between layers is assessed using an infrared (IR) camera, which measures the temperature at the top surface of each layer. This method also enables reconstruction of the vertical temperature distribution along the phantom's z-axis. As an alternative, a vertically split phantom can be used to obtain similar information. An IR camera is strongly recommended because it provides far superior spatial res-

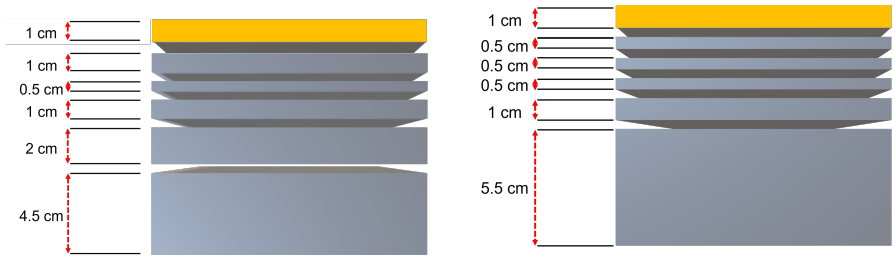

(a) < 915 MHz **(b)** ≥ 915 MHz

Figure 3.2: Phantoms for QA of superficial HT consisting of multiple fat-muscle layered mimicking phantoms. The yellow top layer represents a 1 cm thick fat phantom, whereas the remaining gray layers are muscle phantom

olution compared to discrete temperature probes placed at different phantom depths. A detailed implementation of this procedure is presented in Chapter 4 and in Paper B.

The current guidelines prescribe the following QA metrics:

- Thermal Effective Field Size (TEFS): Defined as the area enclosed by the 50% maximum TR contour at a depth of 1 cm in a muscle-mimicking phantom, directly beneath the applicator aperture.
- Thermal Effective Penetration Depth (TEPD): Defined as the depth at which the local TR reaches 50% of its maximum value (i.e., $\Delta T \geq 3$ °C within 6 min), evaluated at a depth of 1 cm.

TEFS and TEPD are descriptive quantities; therefore, no minimum acceptable values are specified for determining whether a device is adequate. Instead, they serve as comparative indicators for assessing the heating performance of a given applicator and quantify the volume under the applicator aperture which can be effectively heated by the device.

Deep HT The most recent version of QA guidelines for deep HT techniques [34] *(under review)* focuses on phased-array systems. In these devices, power is delivered through an array of equispaced antenna elements that can be controlled independently, allowing flexible shaping and steering of the heat-

ing pattern [77]. According to the guidelines, the performance of such applicators is evaluated through the characterization of the spatial temperature distribution achieved in a standardized QA phantom.

This approach reflects the fundamental objective of HT: to provide heating in a controlled and reproducible way within the target region while minimizing exposure to surrounding healthy tissues. It also marks a shift from earlier guidelines [113], which primarily relied on assessing energy deposition patterns in terms of specific absorption rate (SAR). In contrast, the updated framework emphasizes temperature-based performance indicators, which complement TR and focusing ability. These indicators are quantified through the following metrics:

- Focus center (Fc): The location of the maximum temperature increase within the phantom, expressed in 3D coordinates (C_x, C_y, C_z).
- Focus symmetry (FSym): It is the maximum relative (%) deviation in temperature rise measured at four symmetrically placed catheters ($\pm$x, $\pm$y) around the focus in the axial plane. It quantifies how symmetrically the applicator heats around the intended focus.
- Thermal Effective Field Volume (TEFV): The 3D volume of effective heating, defined by the distances between the inflection points of the temperature profiles along the x-, y-, and z-axes in the phantom. It represents the size of the heated region produced by the applicator.
- Focus steering (FSteer): It is measured as the difference (in cm) between the planned focus location (from the control software) and the experimentally measured maximum temperature position, determined from interpolated temperature data. It describes the applicator's ability to move the heating focus to a user-defined location.

A graphical representation of these quality metrics is shown in Figure 3.3.

The experimental evaluation of these parameters is conducted using standardized phantoms equipped with catheters that house temperature sensors at prescribed locations, allowing the required temperature profiles to be recorded. These phantoms typically consist of a cylindrical hard-plastic container, which to some extent mimics the external fat layer, and contain an internal array of catheters for sensor insertion. The containers are filled with tissue-mimicking

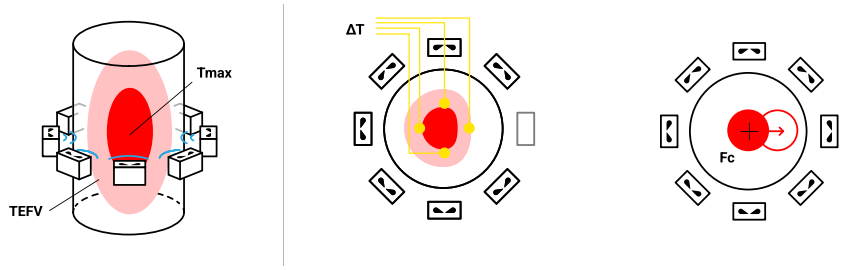

(a) TEFV **(b)** FSym **(c)** FSteer and Fc

Figure 3.3: Graphical representation of the quality parameters used for the applicator characterization according to the new QA protocols for deep HT devices. Adapted from [34].

solutions such as wallpaper paste (WPP) mixtures or agarose-based muscle-mimicking gels. The design rationale of these phantoms is illustrated in Section 3.3.

In addition, the use of phantoms equipped with LED or lamp matrices is recommended prior to the use of tissue-mimicking phantoms, as these enable a rapid, visual assessment of the applicator ability to achieve a central focus and to steer the heating region [119]. These phantoms consist of an array of LEDs or diodes submerged in a saline solution, encased within a cylindrical plastic shell. The saline solution is calibrated to mimic the electrical conductivity of biological tissue, such that the LEDs or diodes illuminate in response to the applied RF field. The resulting luminous pattern is visually inspected to evaluate focusing and steering performance, as illustrated in Figure 3.4. If no central focus or clear steering is observed, adjustments to the applicator phase settings are required.

3.3 QA phantoms development

A tissue-equivalent phantom is defined as a material or structure that replicates the relevant properties of biological tissues for the application of interest. These phantoms are typically composed of a polymeric matrix combined with additional components that fine-tune their physical characteristics to the desired range. For HT applications delivered via EM fields, the phantom ma-

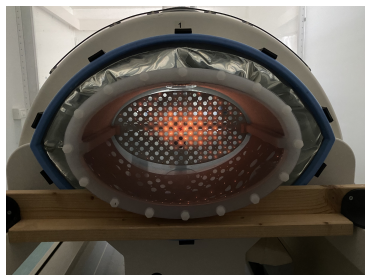

(a) $(x_0, y_0) = (0, 0)$

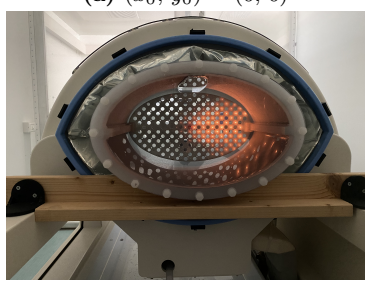

(b) $(x_0, y_0) = (6, 0)$

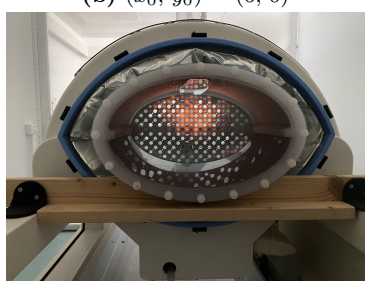

(c) $(x_0, y_0) = (0, 6)$

Figure 3.4: Qualitative evaluation of the steering capability at different locations of the BSD Sigma-Eye applicator (Pyrexar Medical, Salt Lake City, UT, USA) using a custom-built lamp phantom.

terial must meet specific requirements regarding its electrical, thermal, and practical properties [114]:

- **Dielectric properties:** The phantom should closely (or with a reasonable variability) reproduce the dielectric properties of the tissues being emulated.

- **Thermal properties:** Thermal conductivity and specific heat capacity should match target values to approximate the heat distribution in tissue. Mimicking perfusion is generally impractical, as blood flow acts as a strong heat sink.

- **Mechanical stability:** Solid phantoms must retain their structural integrity, even at elevated temperatures, without deformation or material degradation.

- **Long-term stability:** Dielectric, thermal, and mechanical properties should remain stable over time to ensure reproducibility across multiple measurements.

- **Ease of fabrication:** The phantom should be straightforward to manufacture using reproducible procedures.

- **Material accessibility and safety:** Components should be inexpensive, readily available, and non-toxic.

Various phantom materials can be employed for the characterization of HT devices. Phantoms can be broadly categorized into viscous, semi-solid, and solid. Viscous and semi-solid phantoms are primarily utilized to characterize deep HT applicators, while solid phantoms are suitable for deep and superficial HT assessments.

Current solid muscle-mimicking phantoms commonly used in HT QA include sucrose–agar formulations [120] and the so-called superstuff phantom [121]. A well-established semi-solid muscle phantom widely used for evaluating deep HT devices is based on a mixture of wallpaper paste powder and deionized water [114]. This mixture is typically contained within a custom-made plastic container, the design of which will be discussed later in this chapter.

Although several fat-mimicking phantom formulations have been proposed, many suffer from limitations such as complex preparation procedures, inadequate thermal or dielectric properties, or limited long-term stability and short shelf-life. Examples include flour–oil mixtures [122], gelatin gels reinforced with crystalline nanocellulose [123], and water-free "dry" phantoms [124]–[126]. To address these limitations, we propose an alternative fat-mimicking formulation based on an ethylcellulose-based oleogel, which is described in the following section.

Ethylcellulose based fat phantom for superficial HT

Fatty tissue has a substantial impact on electromagnetic wave propagation in superficial HT. Numerical simulations by Kok et al. [81] showed a marked decrease in electromagnetic absorption in a muscle phantom when a superficial fat layer was added, with reductions of approximately 40% for radiative HT and 70% for capacitive HT. These findings emphasize the need for a reliable fat-mimicking material to ensure accurate assessment of superficial HT applicators. Consequently, the lack of an appropriate fat-equivalent phantom poses a significant challenge for implementing superficial HT QA guidelines.

To address the limitations of the available fat-mimicking formulations, we introduce in Paper A a new fat-equivalent phantom based on an ethylcellulose (EC) oleogel composed of a glycerol–oil mixture. EC functions as a matrix-forming agent capable of producing oleogels with high melting temperatures, making EC–glycerol formulations well suited for routine HT QA procedures.

Phantom formulation design

In the proposed formulation, EC acts as a network-forming agent, while the ratio of glycerol and oil regulates the permittivity and conductivity of the phantom, respectively. Because no water is used, the formulation avoids rapid material degradation and exhibits markedly improved long-term stability.

A crucial parameter of EC is its viscosity (or molecular) grade: higher viscosity grades generally produce a more compact and structured polymer network, as illustrated in Figure 3.5. In our case, EC with a viscosity between 41 and 49 mPa·s proved effective. Using EC with a substantially higher viscosity may hinder the mixing process, promote air entrapment, and complicate phantom handling due to excessively rapid solidification.

One of the defining characteristics of fatty tissue is its infiltration into the underlying muscle, i.e., the interspersed growth of adipose cells between muscle fibres. Human fat can exhibit various levels of infiltration, and its dielectric properties consequently vary with the degree of adipose cells–muscle mixing. In the frequency range of 8 MHz to 1 GHz, non-infiltrated fat, due to its low water content, shows relatively low permittivity values (approximately 5–15) and low conductivity values (0.03–0.05 S/m). In contrast, average infiltrated fat exhibits markedly higher permittivity (approximately 11.3–32) and conductivity (0.05–0.11 S/m) due to increased water content and structural heterogeneity [127]. Figure 3.6 illustrates the dielectric properties of both non-infiltrated and infiltrated fat across the relevant frequency range.

Our objective was then to tune the dielectric properties of the phantom so that the material represents the average properties of fatty tissue, falling within the range defined by both infiltrated and non-infiltrated fat. In particular, we aimed to match these properties at 434 MHz and 915 MHz, the two most common operating frequencies for superficial HT applicators. The key parameter governing the dielectric behaviour of the phantom is the glycerol concentration, which strongly influences both the permittivity of the final mixture and its mechanical stability.

As shown by Meaney et al. [128], pure glycerol exhibits a relative permittivity of approximately $\epsilon_r \approx 40$ below 1 GHz, which decreases and plateaus around $\epsilon_r \approx 9$ above 1 GHz. Its conductivity also remains moderate, reaching about $\sigma \approx 0.5$ S/m below 1 GHz. These dielectric properties are plotted in Figure 3.6, together with those of oil and human fat.

To reproduce the desired dielectric characteristics, we tested glycerol concentrations ranging from 50 wt% to 65 wt%. However, rheological assessments revealed that higher glycerol concentrations adversely affect the mechanical stability of the phantom. We therefore identified 57 wt% as the maximum feasible concentration that provides sufficiently high permittivity while preserving acceptable structural integrity. In addition, we developed an alternative formulation with 52 wt% glycerol, better suited for frequencies above 700 MHz, as described in [129].

Two alternative versions of the recipe, targeting frequencies below and above 700 MHz, respectively, are summarized in Table 3.1. The preparation protocol consists of three main steps: (i) creating a glycerol-in-oil suspension, (ii) adding the EC powder, and (iii) pouring the resulting mixture. For complete-

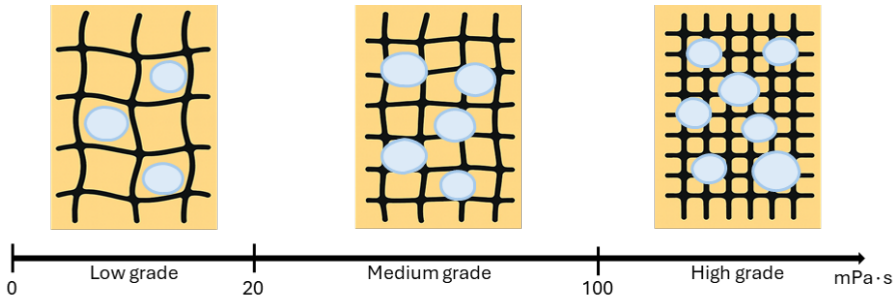

Figure 3.5: Graphical representation of the effect of EC viscosity on the structure of the phantom. The EC forms a polymeric network within the oil phase that traps dispersed glycerol droplets. The density and compactness of this network depend on the EC viscosity grade. Lower-viscosity EC produces a more open, loosely connected structure, while medium- and high-viscosity EC grades generate progressively denser and more structured matrices. Based on these differences, EC can be classified into low (4-20 mPa·s), medium (20-100 mPa·s), and high ($>$ 100 mPa·s) viscosity grades.

ness, the full procedure described in Paper A is provided below.

Detailed procedure

1. Oil and glycerol are mixed at room temperature. A head-mixer with adjustable speed is used for this purpose (ME SH-11-6C, MESE, Leeds, England). Alternatively, any other suitable device can be used. The mixing speed is adjusted so that no air bubbles are visually present. A mixing speed of 420 rpm was selected for a small batch ($\sim$0.3 kg); 1000 rpm, instead, for a larger batch ($\sim$1.2 kg). Higher mixing speeds would determine excessive trapping of air.

Table 3.1: Concentrations of glycerol, EC, and oil for the fat phantom optimized recipe

Frequency range	Glycerol (wt%)	EC (wt%)	Oil (wt%)
$<$ 700 MHz	57	7	36
$\geq$ 700 MHz	52	8	40

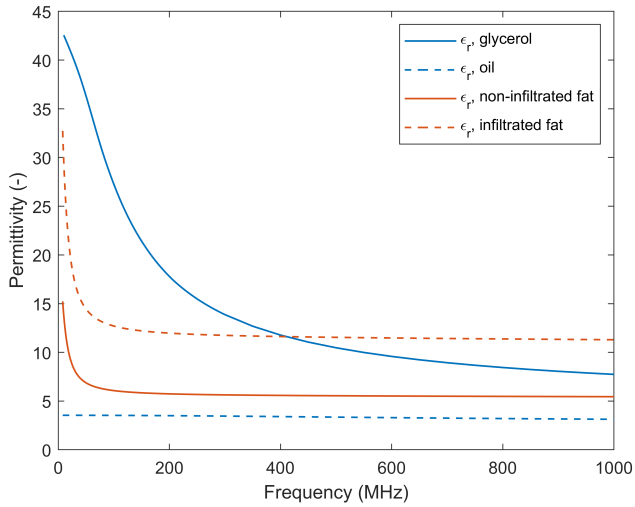

(a)

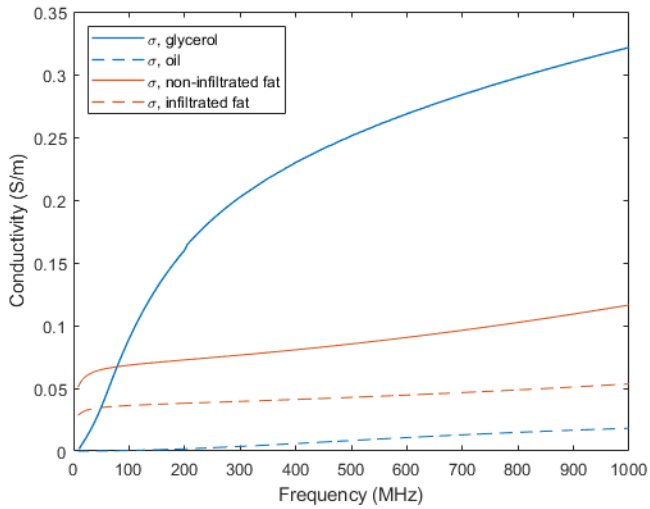

(b)

Figure 3.6: **(a)** Permittivity of average infiltrated fat (orange solid line) and not infiltrated fat (orange dashed line) between 8 MHz and 1 GHz, retrieved from the IT'IS database [127] and permittivity of glycerol (solid blue line) and oil (dashed blue line) measured in the same frequency range; **(b)** Conductivity of fat, oil and glycerol between 8 MHz and 1 GHz. The same colour code as **(a)** is used.

2. Once a visually uniform emulsion is obtained, which takes around 10 min, the temperature is gradually increased to 130 °C . A commercially available hot plate is used. The temperature monitoring can be performed by means of a needle-probe thermometer.

3. The EC is then gradually added to the glycerol–oil mix at 130 °C until EC is visually dissolved. To ensure thorough dissolution, it is recommended to use a spoon to break down any larger clumps. It's crucial to confirm that the EC is evenly distributed within the glycerol-oil suspension. Inadequate mixing may result in the EC floating on the surface, potentially leading to the exclusion of part of the glycerol and oil from the final solid gel.

4. The temperature is now increased to 170 °C to enable the pouring of the compound into the mould without rapid solidification. During this procedure, the pot should be covered to limit the dispersion of hot vapours.

5. The compound is poured into the desired mould and let to cool down. Using heat-resistant gloves is recommended. It is important to pour the compound quickly: if slowly, the mixture might separate.

6. Once the mixture cools down, the phantom can be stored either in a refrigerator or in a dry environment.

Properties assessment and remarks

The resulting material forms a solid yet flexible gel that is straightforward to handle. The dielectric, thermal, and mechanical properties of the phantom were characterized using established methodologies, as detailed in Paper A. Overall, the material exhibits suitable characteristics for superficial HT QA, although some limitations were observed in its conductivity, which remains below the expected values at low frequencies. We attempted to address this problem by adding salt to the formulation, a common strategy for increasing phantom conductivity. Specifically, we tested the addition of table salt (NaCl) and calcium chloride ($CaCl_2$); however, this approach proved unsuccessful. As shown in [128], the effect of these salts in glycerol-based mixtures becomes significant only at frequencies above approximately 300 MHz. Future work should therefore explore alternative salts or ionic additives, although this

remains challenging due to the limited solubility of many such compounds in glycerol.

The applicability of the phantom for assessing superficial HT technologies has been validated both numerically and experimentally (see Paper A). Moreover, its use with low-frequency capacitive devices was recently evaluated in [130], where the phantom demonstrated robust performance during experimental verification.

Deep HT QA phantoms

To experimentally assess the performance of phased-array deep HT devices, the most recent QA guidelines recommend the use of standardized phantoms consisting of an external hard plastic shell (partly mimicking the subcutaneous fat layer) filled with a homogeneous tissue-mimicking material. For reasons of reproducibility and cost-effectiveness, homogeneous phantoms are generally preferred over heterogeneous anthropomorphic or elliptical phantoms. The phantom should also include catheters strategically positioned to accommodate temperature probes. These probes are placed to capture the internal temperature distribution, thereby ensuring a reliable evaluation of the device performance.

The design of a QA phantom typically considers four key parameters:

- Phantom diameter
- Phantom length
- Placement of temperature probes
- Properties of the tissue-mimicking material

The choice of phantom diameter requires balancing patient anatomy, applicator geometry, and the operating frequency. If the diameter is too small compared to the wavelength, forming a well-defined focal point becomes impractical. For deep HT applicators targeting head-and-neck (H&N) and limb tumours, operating at frequencies between 400 and 800 MHz, the corresponding wavelength in muscle-equivalent materials ranges from 5 to 10 cm. For abdominal and pelvic tumours, where frequencies are typically between 70 and 120 MHz, the wavelength increases to approximately 30 cm.

For H&N and limb phantoms, the recommended diameter is 12 cm, corresponding to the average neck diameter in patients with H&N malignancies [131]; this value is also compatible with the expected wavelength. For pelvic and abdominal applicators, the selected phantom diameters are 25 cm for devices operating around 100 MHz and 31.5 cm for devices operating at lower frequencies, typically near 75 MHz.

Phantom design

The choice of phantom dimensions, material properties, and probe positioning is guided by electromagnetic–thermal simulations performed with multiphysics solvers. The influence of catheters and catheter-holding structures on field propagation and temperature distribution is also evaluated numerically.

A robust simulation setup should include several elements to ensure a reliable design process:

- Selection of clinically relevant frequency points for the treatment area under consideration.
- Use of an applicator model that accurately reproduces all EM-relevant characteristics of the physical device, including antenna geometry (length, shape, number, and spacing) and a water bolus of sufficient thickness to prevent excessive reflections toward the antenna elements.
- Application of an adequate total input power, taking into account the phantom dimensions.
- Use of a suitable tissue-equivalent material.

To define the optimal phantom length, a parameter sweep is performed, in which the phantom length is varied and the resulting SAR distributions are evaluated. This approach allows to assess how the length influences standing-wave formation. In general, excessively short phantoms produce edge hotspots due to standing-wave effects, whereas overly long phantoms become impractical to handle experimentally.

An example of this process is the development of a H&N and limb phantom described in [129]. In that work, we tailored the design for applicators operating at higher frequencies (400–800 MHz), and the external phantom shell was constructed from PVC tubing with a diameter of 12 cm.

The design process was supported by coupled electromagnetic–thermal simulations conducted in CST Microwave Studio (Dassault Systèmes SA, Vélizy-Villacoublay, France). The applicator model consisted of ten bow-tie antenna elements arranged in a circular configuration [90], [132], while the phantom was represented as a homogeneous, muscle-equivalent medium.

For this case study, we identified a length of approximately 50–60 cm as optimal, providing a balance between minimizing unwanted reflections and maintaining experimental usability.

Probe positioning is determined by analysing the SAR and temperature profiles along the x- and y-axes on the central transverse plane. The goal is to capture the spatial gradients generated by the applicator, enabling accurate localization of the focal region and identification of potential hotspots. One probe must therefore be placed at the point of maximum SAR (and, in a homogeneous phantom, maximum temperature). In this example, we positioned one probe at the centre (x = 0 cm) to measure the maximum temperature rise, as shown in Figure 3.7.

Additional probes are placed at the inflection points of the SAR or temperature profiles, which define the edges of the central focus and the onset of wall hotspots. Accordingly, we positioned two probes at 3 cm and 5 cm. To better characterize the focal gradient, we placed two more probes at 1 cm and 2 cm from the centre. Placing additional probes along the orthogonal axis provides information on field symmetry and allows detection of potential off-axis hotspots.

A similar simulation-driven design approach was subsequently extended in Paper B to the development of a WPP phantom intended for larger applicators targeting abdominal and pelvic deep HT. This study employed COMSOL Multiphysics (COMSOL AB, Stockholm, Sweden) and used a simplified model of the BSD Sigma 60, one of the most widely adopted phased-array applicators, as case-study model. The simulation setup is shown in Figure 3.8. Simulations were performed at two clinically relevant frequencies, 75 MHz and 100 MHz, using homogeneous cylindrical phantoms with diameters of 25 cm and 31.5 cm, and the impact of different phantom properties and dimension was examined through parametric analysis. For more details, see Paper B.

The choice of dielectric properties for the phantom filling material represents a critical design parameter. Although the standard phantoms formulations are typically designed to match the dielectric properties of muscle tissue

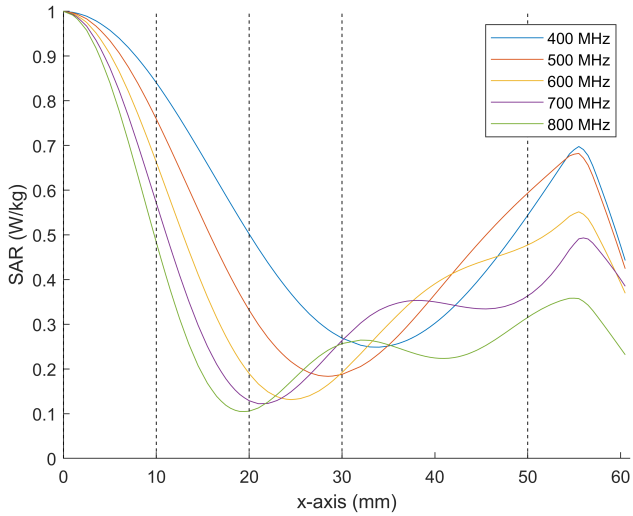

(a)

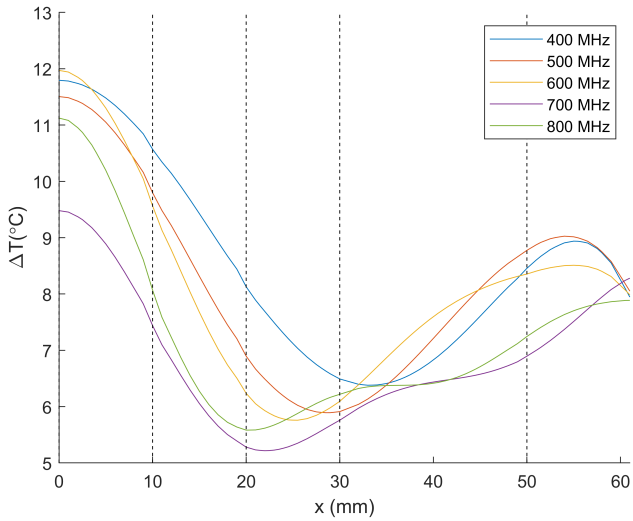

(b)

Figure 3.7: **(a)** Normalized SAR distribution along the x-axis at a H&N phantom central transversal plane for different frequencies. The phantom diameter is 12 cm. The black dotted lines represent the final position of the measuring probes; **(b)** Corresponding temperature distribution after 10 min heating with a total forward power of 150 W.

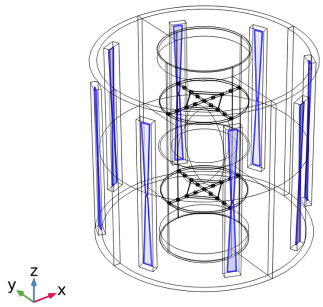

Figure 3.8: Simulation scenario used for the dimensioning of deep HT WPP QA phantom. Applicator, water bolus and phantom are visible, as well as the catheters holding structures.

(conductivity ≈ 0.66 S/m and relative permittivity 77.7 at 100 MHz), it can be argued that the phantom should instead reflect the composite properties of the anatomical region being modelled. Waves targeting abdominal and pelvic tumours penetrate a heterogeneous mixture of tissues (muscle, fat, and bone) many of which exhibit substantially lower conductivity than muscle. Consequently, a phantom based solely on muscle properties may overestimate the effective electrical conductivity of these anatomical regions. A practical approximation is to consider an effective tissue mixture with a conductivity of roughly two-thirds that of muscle, yielding a target value of about 0.44 S/m at 100 MHz. Using this conductivity provides a well-defined focal target at the phantom center for the frequency range considered (75–100 MHz) and for both phantom diameters (25 cm and 31.5 cm), making it particularly suitable for QA purposes.

On the other side, as demonstrated in Paper B, gel conductivities closer to muscle-like values enable the phantom to reproduce heating patterns observed in realistic patient models. This highlights the importance of clearly defining the intended purpose of the phantom. If the primary aim is QA—specifically, maximizing thermal-gradient resolution to support performance benchmarking—a lower conductivity may be preferable. In contrast, if the goal is to approximate clinically realistic heating distributions, a higher conductivity consistent with muscle tissue may provide a closer representation of patient behavior, even if with reduced sensitivity to spatial gradients.

CHAPTER 4

Hyperthermia QA protocols: experimental implementation

Translating HT QA guidelines into clinical practice is challenging due to a wide range of uncertainties related to the existing variability of phantom materials and heating and monitoring devices. This chapter focuses on the experimental QA assessment of superficial and deep HT applicators, which allows us to point out the factors affecting the practical implementation of the guidelines. We have adopted the latest QA protocols, which involve the evaluation of quality parameters based on temperature measurements.

4.1 Superficial HT QA assessment

In Paper C [133], we present the QA verification for superficial HT [32] of the lucite cone applicator (LCA) using the most recent ESHO-QA guidelines. The LCA has been used as a standard device for the treatment of breast cancer recurrences at Erasmus Medical Center, Rotterdam, The Netherlands. This represents the first attempt to experimentally assess a clinically employed superficial HT device using temperature-based metrics. In addition, we created

an equivalent computational model of the device and QA experimental setup to compare with the experimental results.

Experimental procedure

The LCA is shown in Figure 4.1 and consists of a 434 MHz water-filled horn applicator with a square aperture of 10×10 cm^2. Up to six different antenna elements can be combined to treat a total area of 600 cm^2, with independent temperature control for each antenna element.

The LCA QA measurements were performed by evaluating the temperature increase distribution in a layered fat-muscle phantom manufactured following the QA guidelines reported by reference [32]. The phantom consisted of a 1-cm thick phantom layer with fat-mimicking properties overlaying a muscle-mimicking phantom with an overall thickness of 9 cm. The muscle layer was further subdivided into five different layers, as shown in Figure 3.2a. The fat-mimicking layer was produced according to Paper A, while the muscle phantom was based on a superstuff-agar mixture and prepared according to the guidelines [32]. Dielectric and thermal properties of the phantom were verified to be tissue-representative, as explained in paper C.

Six antenna elements were evaluated individually, and then in 2×1 and 2×2 array configurations, using the same experimental setup. Each LCA antenna was driven by a 434 MHz generator through a bidirectional coupler, and forward and reflected powers were measured with a power meter. Coupling to the phantom was achieved using a 2-cm deionized water bolus, with lateral dimensions adapted to the antenna arrangement. Water circulation in both the bolus and antenna horn ensured stable temperature conditions. A picture of the experimental setup is shown in Figure 4.1.

In each experiment, power was applied for 6 minutes, with transmitted and reflected powers reported in Paper C. A multi-sensor fibre-optic probe measured the temperature at 1 cm depth beneath the centre of the antenna aperture to verify the required temperature rise (6 °C in 6 min). After heating, the antenna(s) and water bolus were removed, and the temperature distribution was recorded using a thermal IR camera mounted above the phantom. Temperature maps were acquired sequentially by removing one phantom layer at a time, from 0 cm to 5.5 cm depth. Numerical evaluation showed that heat diffusion during the ≈60 s acquisition process was negligible.

The heating experiments were replicated numerically using the Sim4Life

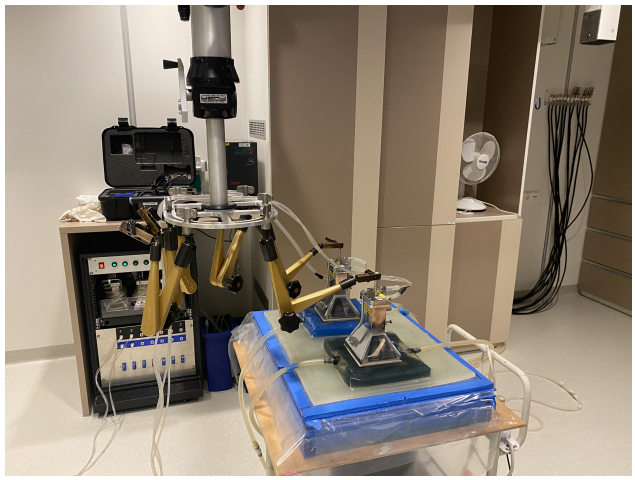

Figure 4.1: Experimental setup used for the assessment of LCA antennas.

software package (v5.2, Zurich MedTech AG, Zurich, Switzerland). Coupled electromagnetic–thermal simulations were performed using a finite-difference time-domain solver. The QA metrics prescribed by the guidelines, TR, TEFS, and TEPD, were computed from the simulated temperature distributions for both phantom models, enabling a quantitative comparison. Additional details and results of the experimental–numerical comparison are provided in Paper C.

Challenges in the superficial HT guidelines application

The knowledge acquired during the practical application of the superficial HT guidelines and the following comparisons with numerical results offer valuable insights that are shared here to facilitate the translation of QA guidelines into clinical practice. This attempt was the first documented effort to apply the new QA guidelines for superficial HT applications to a radiative device currently in clinical use.

The aim of this research was to reveal the major limitations and challenges while implementing superficial HT guidelines. This is especially relevant considering the expected constraints that can arise from the limited availability of QA equipment in a typical clinical environment:

Phantom manufacturing: The availability of high-quality tissue-mimicking phantoms is essential for the QA assessment of HT devices. Uncertainties in phantom properties or structural inhomogeneities can significantly affect evaluation outcomes—as demonstrated in Paper C, where experimental results were compared with simulations performed on two phantom models: a simplified "geometrically perfect" layered model and a realistic model obtained by segmenting a CT scan of the manufactured phantom. To minimize such uncertainties, the manufacturing process of QA phantoms must be as simple and as reproducible as possible. In the case of the layered phantom used for the LCA evaluation, producing layers of superstuff–agar muscle phantom posed notable challenges. The high viscosity of the mixture made air entrapment unavoidable, and achieving uniform layer thickness during casting was difficult. A metallic flat tool was used to smooth the surface after pouring the mixture into casting frames, but this procedure could not guarantee the desired accuracy, leading to unavoidable air pockets between layers. A practical solution is to employ a different phantom material, such as a sucrose–agar mixture. This formulation offers versatile dielectric properties that can be tuned by adjusting the sucrose-to-salt ratio [120]. Moreover, the mixture stays liquid immediately after preparation and solidifies over the following 24 hours, making the casting process far more manageable, since simply pouring the mixture into the mould is sufficient.

Time constraints: The entire experimental procedure was over three weeks, including approximately one week dedicated to phantom preparation. We conducted eight experiments in total, consisting of six individual antennas and two antenna-array configurations. A 12-hour interval was maintained between consecutive experiments to allow the phantom to fully re-equilibrate to room temperature. Additional time was required for antenna calibration to minimize power reflections. Beyond the experiments themselves, it was also necessary to account for the possibility of repeating measurements due to execution errors. Altogether, these factors resulted in a substantial time commitment, which may be difficult to accommodate in a clinical setting. However, the QA workload in other institutions is expected to be considerably lower, as most HT centres use commercial devices with one or two antenna elements. In contrast, Erasmus Medical Center employs a more complex in-house–developed array consisting of 2–6 elements. As a result, the evaluation process at institutions using commercial applicators would

likely be considerably faster due to the lower number of antenna elements.

Temperature measurement: The evaluation of temperature distribution is challenging due to many influencing factors, including the temperature of the water bolus and the precise positioning of the applicator. When not complemented by temperature sensors, thermal camera measurements may not provide a comprehensive assessment of the temperature distribution generated by the applicator. To reduce uncertainties and obtain a more reliable assessment, additional temperature probes placed at multiple depths within the phantom should be considered.

Additional evaluations: Although the QA guidelines provide only the essential requirements for evaluating superficial HT applicators, additional measurements can be highly valuable for achieving a comprehensive physical characterization. These may include determining the efficiency of individual antenna elements, assessing the heat transfer coefficient of the water bolus, or quantifying the impact of antenna placement and bolus thickness, factors shown to significantly influence heating patterns and temperature uniformity. As demonstrated in Paper C, careful control of these parameters is crucial: deviations in antenna tilt or inconsistencies in bolus thickness can markedly alter EFS distributions, making comparisons across studies difficult.

The first experimental application of the new superficial HT QA guidelines to a clinically used radiative applicator shows that reliable QA requires more than meeting the prescribed temperature-based metrics. The study demonstrates that phantom quality, antenna positioning, bolus thickness, and careful temperature measurement critically influence the outcome of QA evaluations. Numerical modelling further highlights that realistic phantom geometry and properties are essential to reproduce experimental behaviour. Together, these findings show that effective clinical implementation of superficial HT QA demands simplified phantom manufacturing, consistent experimental setups, and, where feasible, supplementary measurements that go beyond the minimum guideline requirements.

4.2 Deep HT QA assessment

Facilitating device-independent and multi-institutional studies is a key motivation for developing standardized QA guidelines in hyperthermia. Although

QA procedures are broadly performed, substantial variation persists across institutions regarding how these protocols are implemented. Standardization therefore holds significant value in enabling reproducible, comparable, and clinically meaningful assessments. With this objective, Paper D [134] presents a comprehensive comparative study involving six HT centres in Germany and the Netherlands. The study aimed to verify the feasibility of temperature-based QA procedures for deep HT, document practical aspects related to system setup, and quantify the time required to perform the protocol. The outcomes provided critical insights that were subsequently incorporated as recommendations in the most recent deep hyperthermia QA guidelines, currently under review [34]. Device performance was assessed using temperature rise (TR) and temperature-based quality metrics, including focus location and focus symmetry, evaluated in a homogeneous QA phantom with clinically used thermometry systems, thereby ensuring that the protocol can be directly integrated into routine QA workflows. Details on the measurement campaign and detailed results can be found in paper D.

Status quo of QA procedures for deep HT

Only about 30% of centres verified heating and steering capability at the recommended frequency of every 1–3 months, while most performed these checks far less frequently, in some cases only once per year or less. Approximately 70% of centres relied on LED/lamp phantoms or solid phantoms equipped with catheters for routine QA, while others used E-field probes or anthropomorphic phantoms. Common phantom materials included agarose-based formulations and WPP gels. Despite the widespread use of phantoms, fewer than 20% of centres had access to dielectric or thermal properties measurement equipment, and even when available, phantom properties verification was rarely performed.

Heating protocols also varied considerably: although most centres applied heating for 10–15 minutes, both power settings and the expected temperature-rise thresholds differed widely. Phantom positioning practices showed similarly large variation, including the use of foam supports, dedicated holders, or direct placement on the patient table—variability that, as shown later, likely affected measurement reproducibility. Calibration routines were inconsistent as well. Only 40% of centres calibrated thermometry before each QA test, and bolus water conductivity checks ranged from monthly to never.

Despite these differences, all centres evaluated TR, and most of them additionally assessed heating symmetry or applicator efficiency, indicating partial adoption of temperature-based QA metrics.

Overall, the findings highlight the need for more harmonized procedures. Differences in phantom properties, positioning workflows, and measurement techniques currently limit inter-centre comparability and reinforce the importance of establishing clear, standardized QA protocols for deep HT.

Challenges in deep HT QA guidelines application

During the campaign, we performed a total of 54 measurement repetitions (for details, see Paper D). The experience gained from this work provided several insights into the feasibility and practicality of the QA guidelines for deep HT, particularly in an inter-institutional context.

Accuracy of thermal mapping and its verification

All participating institutions relied on a thermal mapping system for temperature measurements, in which the probes are mechanically moved along the catheter in fixed steps by a dedicated positioning device. One of the main challenges identified with this system is the considerable variation in its performance across institutions, which strongly affects the reliability of the measured temperature profiles. Positional inaccuracies were common, typically around 2 cm, and became more pronounced when multiple probes were used simultaneously. As further demonstrated in Paper B, inaccuracies of up to 4 cm were observed as the number of probes increased.

To evaluate this effect more systematically, we conducted a dedicated investigation using two BSD 2000 DHT systems equipped with Sigma 60 applicators and standardized QA phantoms at two different institutions. A structured four-step procedure was followed:

1. Probes were calibrated in a temperature-controlled water bath, achieving an uncertainty of ± 0.2 °C.

2. Thermal mapping positional accuracy was assessed through dry runs using transparent catheters marked at 1 cm intervals over a 25 cm range, enabling construction of calibration curves (Figure 4.2).

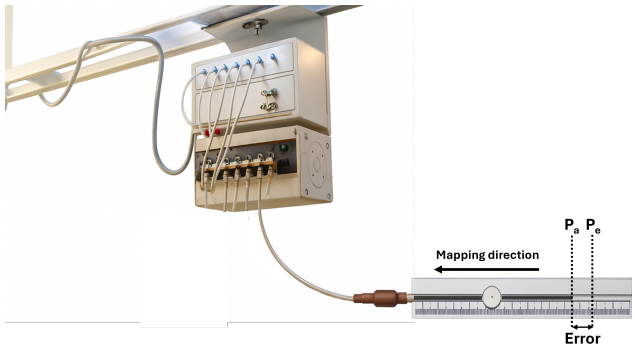

Figure 4.2: Verification procedure of the thermal mapping system. The probe is retracted inside a transparent catheter, and its actual mapping position (P_a) is measured with a ruler and compared to the expected position (P_e), allowing the determination of the corresponding mapping error.

3. A standard QA experiment was conducted according to the recommended protocol.

4. Measured temperature distributions along the central z-axis at $(x, y) = (0, 0)$ were compared with corresponding numerical simulations.

The results showed a clear deterioration of mapping accuracy with increasing number of probes. When two probes were used simultaneously, the average positional error was 1.0 ± 0.1 cm. With four probes, the error increased to 3.8 ± 1.0 cm. The resulting calibration curves (Figure 4.3) illustrate how additional probes lead to greater deviations and reduced reproducibility.

These findings were further confirmed in QA experiments using both cylindrical and elliptical phantoms. With two probes, agreement between measured and simulated temperature distributions was excellent, with an average difference of $0.2 \pm 0.1\,^{\circ}\mathrm{C}$. In contrast, with four probes the discrepancy grew to 0.7 $\pm$ 0.5 °C. Moreover, measurements with more than two probes required continuous visual inspection and manual adjustments to maintain proper probe tension and positioning.

The results of the multi-institutional study revealed the significant impact of probe-movement inaccuracies in thermal mapping, underscoring the need for a dedicated verification step. Thermal mapping systems must always be checked using dry-run tests with marked catheters prior to QA procedures

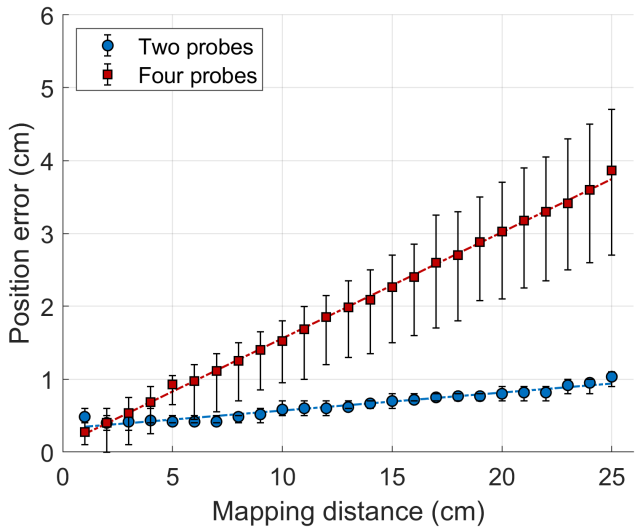

Figure 4.3: Calibration curves of the BSD-2000 thermal mapping system. The plots show the probe positioning error, defined as the difference between the actual and expected probe position along the marked catheter, across the mapping range. Results are presented for measurements performed with two and four probes simultaneously, including their associated variation.

or clinical use. This procedure allows the generation of calibration curves that compensate for systematic mapping errors. Dry-run verification must be complemented by probe calibration in a temperature-controlled water bath. Moreover, for QA applications, no more than two probes should be used simultaneously, as this ensures reliable and reproducible measurements.

These verification procedures could not be implemented during the campaign due to practical constraints. The study was limited to three weeks, with only about two days available at each centre, leaving insufficient time for detailed system checks. Several probe-related issues could likely have been mitigated with additional preparation.

Phantom positioning

The phantom position within the applicator substantially influences the resulting temperature profiles. As demonstrated in Paper B, misalignment of the phantom along the x-, y-, or z-axis relative to the applicator centre can produce temperature deviations of up to 2 °C. Because phantom positioning is performed manually, the risk of misplacement is inherently high. The use of dedicated positioning supports to ensure that the phantom is secured at the vertical centre of the applicator is therefore essential. In addition, alignment aids, such as laser guides or other positioning tools, are strongly recommended to ensure correct placement along the x- and y-axes. Pairwise verification is advisable when manually measuring the distance between the phantom and the applicator frame, as this helps minimize operator-dependent errors. Care must also be taken during bolus filling: the weight of the water bolus can cause the phantom to shift. For this reason, rechecking the phantom position after the bolus has been filled is recommended.

Quality metrics definition

The investigated systems were evaluated using the metrics defined in the most recent QA guidelines [34] (under review). These metrics were originally formulated based on expected heating patterns in homogeneous phantoms, supported primarily by simulation studies rather than extensive experimental validation. While some parameters such as TR, focus location, and focus symmetry were relatively straightforward to determine from the measured axial temperature profiles (see Paper D for details), the application of the

TEFV proved challenging in its original form.

Originally, TEFV was defined as the volume within a homogeneous phantom enclosed by the 75% maximum temperature-rise contour, i.e., the region where the temperature rise reached at least 4.5 °C for a target TR of 6 °C. In practice, this corresponded to an ellipsoidal volume whose X–Y cross-section was determined from radial probe measurements falling below the 75% threshold (Figure 4.4a). However, the experimental data showed that this assumption did not consistently hold: hotspots generated by conductive heat transfer near the phantom wall often maintained temperatures above the 75% threshold, preventing the contour from closing as required by the original definition. Therefore, the parameter had to be revised.

Based on observations collected during the campaign, the TEFV has been redefined as the ellipsoidal volume characterized by three axial dimensions, L_x, L_y, and L_z, describing the extent of the heated region in a uniform QA phantom. The dimensions L_x and L_y are derived from the inflection points of the temperature profiles along the x- and y-axes, identified via the second derivative of the curves measured by the radial probes on the phantom's X–Y plane (Figure 4.4b). The average temperature at these inflection points, T_{infl}, is then used as a reference to determine L_z, defined as the distance between the two points along the z-axis where the temperature equals T_{infl}. If only half of the longitudinal temperature profile is available, L_z is estimated by doubling the distance from the inflection point to the focus centre coordinate C_z.

Updated QA protocol

Taking into account the limitations imposed by the available instrumentation, together with evidence from practical experience, we derived a recommended measurement setup to account for system- and experiment-related inaccuracies. The main steps required to perform a QA experiment in deep HT can be defined as follows:

1. **Thermometry verification:** All thermometry probes planned for use in the experiment must be calibrated, preferably in a temperature-controlled water bath using a reference sensor. If a thermal mapping system is used, its positional accuracy must be verified through a dry run in a marked catheter. The resulting calibration curve should be

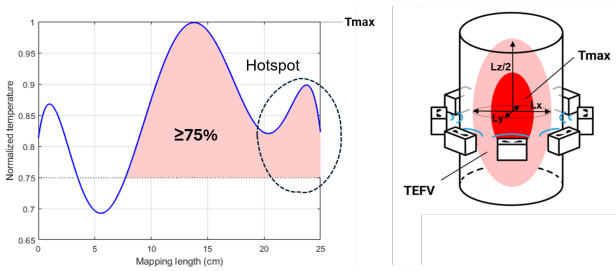

(a) TEFV calculation method based on the 75% isoline definition

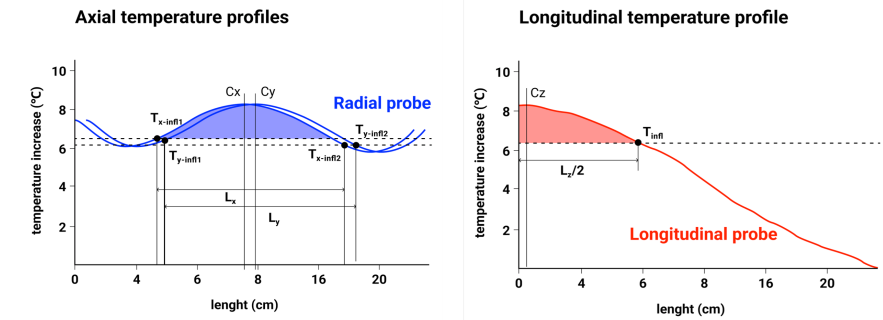

(b) TEFV based on inflection points

Figure 4.4: Graphical representation of the two definitions for TEFV. **(a)** TEFV as volume defined by the 75% isoline. If a hotspot is present, as in the example shown, the base area of the ellipsoid cannot be defined. **(b)** TEFV based on the lengths defined by the inflection points. This definition holds even in the presence of hotspots.

applied subsequently to correct the recorded temperature profiles.

2. **Phantom positioning:** The phantom must be carefully positioned inside the applicator. Its vertical position should be secured using dedicated holders. Alignment along the x- and y-axes should preferably be verified using laser-guidance systems or equivalent tools. Positioning along the z-axis can be checked by measuring the distance between the phantom edge and the applicator frame with a measuring tape. Peer verification is strongly recommended.

3. **Probe positioning:** The probes are inserted into the catheters according to the planned experiment (central or shifted focus). It is recommended to verify that each probe tip is located at the expected position. This can be done by marking the correct insertion depth on the probe and inserting it until the marker aligns with the catheter entrance. To improve the accuracy of focus localization and temperature mapping, the use of five probes is advised. This configuration provides additional measurement points for curve fitting, thereby reducing uncertainty in estimating the focus location. The recommended setup is as follows:
   - For central focus: three longitudinal probes placed at (0,−3), (0,0), and (0,3) cm along the main axis.
   - For eccentric focus: three longitudinal probes placed at (0,0), (0,−3), and (0,6) cm along the main axis.
   - Two radial probes.

4. **Bolus filling:** The water bolus is filled and the water temperature is recorded. Care must be taken to ensure that the phantom does not move during filling; if displacement occurs, its position must be corrected and re-verified.

5. **Heating procedure:** The heating process is carried out in three phases:
   - *Baseline acquisition:* If thermal mapping is used, a baseline scan is performed. Otherwise, temperatures are recorded for 1 minute using static probes.
   - *Heating phase:* Heating is applied at 1000 W for 10 minutes. The temperature at the phantom centre (or at the steering location) is monitored. If the temperature rise does not reach 6 °C within

10 minutes, the experiment must be repeated with higher power (after verifying that antenna reflections remain within acceptable limits). When using a steered focus, steering to a target location of (0, 3) cm is recommended, as this represents a clinically relevant displacement and minimizes interference from the phantom wall. If only three probes are available, the focus may be steered to (3, 3) cm, or alternatively, the phantom can be rotated so that a radial catheter intersects the steered focus at (0, 3) cm.

- *Post-heating temperature acquisition:* If mapping is used, a second scan is performed after heating. Otherwise, temperatures are recorded with static probes immediately after power-off. If a clear focus shift from the expected location is observed, the system should be checked with a lamp phantom for rapid verification of steering performance.

6. **Data analysis:** The recorded temperature profiles are processed using any suitable data-analysis tool to compute the required quality metrics. If mapping data are used, the profiles must be corrected according to the thermal-mapping calibration curves prior to further analysis.

A notable limitation of this procedure is the time required between successive measurements. Due to thermal equilibration constraints, a minimum waiting period of approximately five hours is needed for the phantom to return to baseline temperature before a new measurement can be performed. This requirement imposes practical restrictions on the number of measurements that can be completed within a given time frame and should therefore be taken into account when planning experimental QA procedures.

Identified thresholds for QA measurements

Despite a rigorous measurement procedure, non-systematic errors and residual uncertainties related to the device, thermometry, and the phantom may still arise during system verification. This issue is particularly relevant when repeated measurements are not feasible because of the aforementioned time constraints, which might be incompatible with routine clinical workflows. For this reason, we established the following tolerance criteria, which provide confidence that the device is performing correctly, even in the presence of unavoidable uncertainties:

- Minimum temperature increase of $\geq$ 6 °C within 10 minutes ($\pm$0.4 °C deviation).
- Focus location accuracy within $\pm$2.0 cm of the intended target.
- Focus symmetry within $\leq$ 10%, corresponding to a maximum temperature difference of $\pm$0.8–1.0 °C depending on the evaluation method.

More details on these can be found in paper D. These thresholds, together with the experimental recommendations introduced above, have been incorporated into the current QA guidelines, thereby enhancing their robustness and supporting reproducibility in multi-institutional QA of deep HT systems.

CHAPTER 5

Regulatory aspects in HT and the link to QA guidelines

The European Medical Device Regulation (MDR 2017/745) was developed to ensure the safety and performance of medical devices within the EU market [135]. Despite the improvements in safety and transparency achieved by the MDR, it currently imposes substantial operational, financial, and structural burdens on medical device developers [136]. This is particularly relevant in the HT field, where most technological innovation originates from research institutes or small- and medium-sized enterprises, which often lack dedicated in-house regulatory expertise and must consequently outsource these activities. Moreover, developing an HT system is especially challenging from a regulatory perspective, as it requires the integration of multiple interconnected subsystems, as shown in Figure 2.4, both hardware (signal generation and amplification, applicator, thermometry) and software (treatment planning and monitoring) into a single device that must deliver treatment both effectively and safely.

The MDR process starts with defining the conformity pathway, illustrated in Figure 5.1, which consists of the sequence of regulatory steps a manufacturer must follow to legally place a medical device on the EU market. The details of this pathway are described in Section 5.1. Although all these steps are re-

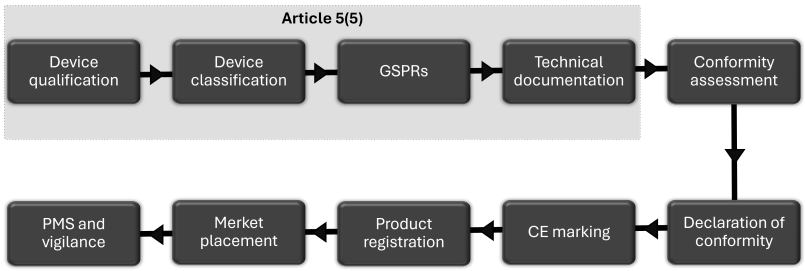

Figure 5.1: MDR conformity route: the main steps are delineated, with the steps relevant under the Article 5(5) in-house exemption highlighted. The upper pathway indicates which regulatory obligations remain applicable for in-house manufactured devices (device qualification, classification, and compliance with GSPRs), while the lower pathway shows the additional steps required for full MDR conformity leading to CE marking and market placement.

quired for a commercially developed device, the process is partially simplified for in-house manufactured medical devices used exclusively within a health institution. For these cases, the MDR includes a specific provision—Article 5(5)—that enables their development and clinical use without undergoing the full conformity assessment process. Devices manufactured under this exemption are not CE-marked, provided that strict conditions are met. This results in a somewhat simplified regulatory route, as shown in Figure 5.1.

In Paper E, this simplified pathway under Article 5(5) is described in detail for external phased-array HT systems, offering comprehensive guidance on navigating the MDR framework in the context of HT.

Once the MDR conformity route is defined, the next step is to understand how to translate it into the practical development of a medical system. For an HT system this represents a particular challenge, given the complex and tightly integrated structure of its subsystems. Two examples of well-established systems (engineering frameworks) that can be adopted are the V-model (or V-scheme) [137] and the Waterfall model [138].

The V-model, illustrated in Figure 5.2, consists of two complementary branches: the left branch translates clinical needs into increasingly detailed design inputs, while the right branch maps these inputs to their corresponding verification and validation activities. Further details on the V-model are

provided in Section 5.2. The Waterfall model, by contrast, is a linear, sequential development approach in which each phase must be completed before the next begins. Although it offers clear structure and documentation, it provides limited flexibility, and for this reason the V-model is adopted in this chapter.

Following the V-model also clarifies how QA procedures integrate into the MDR framework. QA supports device commissioning, a fundamental step that follows regulatory compliance and must be completed before clinical verification of the device can take place. In practice, while the MDR defines the conformity pathway—specifying *what* must be ensured from a safety and performance perspective—QA guidelines define the commissioning procedures, describing *how* these requirements are assessed, monitored, and maintained throughout the device lifecycle.

5.1 Standard MDR path for HT systems

The regulatory workflow applicable to any medical device in the EU can be adapted to the specific requirements of HT systems. The main steps are summarised below:

Device qualification and classification: The regulatory process begins with determining whether the product meets the MDR definition of a medical device, based on its intended purpose and mode of action (Article 2). Once confirmed as a medical device, it must be classified using the rules in Annex VIII, ranging from Class I (low risk) to Class III (high risk). Classification determines the level of regulatory assessment and whether Notified Body (NB) involvement is required. HT systems qualify as medical devices because they deliver controlled thermal energy for therapeutic purposes. They are typically classified under Rule 9 or Rule 11 as active therapeutic devices, placing them in Class IIb. Applicators or probes may fall under Rules 9, 5.4, or 5.5, depending on invasiveness and their connection to the active device. Almost all such components require NB involvement.

Compliance with General Safety and Performance Requirements (GSPRs): All devices must comply with the GSPRs outlined in Annex I of the MDR. These requirements cover essential aspects such as quality management (ISO 13485:2016), electrical and electromagnetic safety, electromagnetic compatibility, usability, safety, and performance. Additional

component-specific requirements may apply, including biocompatibility (i.e., for water bolus), software lifecycle management (i.e., treatment planning and control software), and others. A list of these standards is also detailed in Paper E.

Technical documentation: Manufacturers must compile technical documentation in accordance with Annex II and Annex III, including device description, intended purpose, design and manufacturing information, risk management (ISO 14971), verification and validation results, the clinical evaluation, and the post-market surveillance (PMS) plan. In Paper E, we outline the structure and content of such documentation for an HT system, highlighting subsystem-specific requirements.

Conformity assessment and Notified Body involvement: All devices in Classes Is, Im, Ir, IIa, IIb, and III require assessment by a NB. For a Class IIb HT system, conformity assessment typically follows Annex IX (QMS audit + design examination) or the Annex X/XI routes. Upon successful assessment, the manufacturer issues a Declaration of Conformity and affixes the CE mark. The system, its applicators, and accessories must then be registered in EUDAMED and assigned UDI codes before they can be legally placed on the EU market.

Market placement and post-market surveillance: Once an HT system is authorised for market placement—through EUDAMED registration, UDI assignment, and compliant labelling—the manufacturer must maintain continuous oversight of the device in clinical use. This includes fulfilling all PMS, vigilance, and documentation-update obligations to ensure sustained safety and performance throughout its lifecycle.

Exception: Article 5(5)

Article 5(5) provides an alternative regulatory pathway for health institutions, enabling them to manufacture, modify, and use medical devices within their own facilities without undergoing commercial distribution or full MDR conformity assessment. This exemption is dedicated to hospitals and university medical centres that require bespoke HT devices—such as customised applicators, phantoms, prototypes, or software tools—for clinical or research purposes when no suitable CE-marked device meets their needs.

Conditions to apply Article 5(5)

- The institution must justify why no equivalent CE-marked device is clinically appropriate
- The device must not be produced on an industrial scale
- A publicly accessible statement must be published confirming compliance with Article 5(5)
- Documentation must be made available to competent authorities upon request and
- Appropriate internal PMS and vigilance systems must be maintained.

Although Article 5(5) removes the market-access requirements of the MDR, it does not exempt health institutions from ensuring device safety. Institutions must still:

- Comply with all relevant GSPRs
- Maintain adequate technical documentation,
- Perform risk management, verification, and validation,
- Conduct a clinical or technical evaluation appropriate to the device's intended use
- Operate under an institutional quality management system appropriate for in-house manufacture.

In contrast with standard commercial manufacturers, institutions operating under Article 5(5):

- do not undergo Notified Body assessment;
- do not issue a Declaration of Conformity;
- do not affix the CE mark;
- and do not register the device in EUDAMED or assign a UDI.

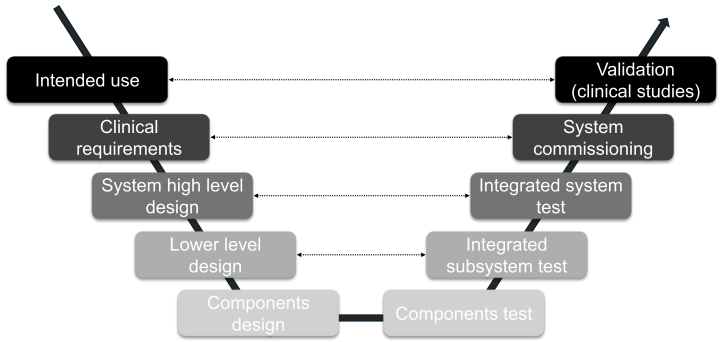

Figure 5.2: V-model representation of the MDR-compliant development process for an HT system. The left branch outlines progressively detailed system and subsystem requirements, while the right branch maps the corresponding verification and validation steps needed to demonstrate conformity.

These exemptions significantly reduce the regulatory burden while still ensuring that in-house HT devices remain safe and capable of fulfilling their intended purpose.

5.2 HT system development according to MDR

As already introduced, the V-model (Figure 5.2) is particularly well suited for the development of HT systems, whose subsystems are tightly integrated. It provides a structured framework for demonstrating that an HT system is safe, reliable, and fit for its intended purpose. The model applies both under the standard MDR conformity pathway and under the Article 5(5) in-house exemption. The key difference lies only in documentation and regulatory oversight: commercial manufacturers must present the V-model outputs for assessment by a Notified Body, whereas institutions operating under Article 5(5) may adapt the level of detail and format of documentation to internal clinical needs while still ensuring full compliance with all technical safety requirements.

On the *left branch* of the V-model, the development begins with defining the intended use and the clinical or user requirements. For HT systems, these include the therapeutic objective of achieving preferential heating in

the target—establishing a focal region while sparing surrounding healthy tissues—minimum heating efficacy, safety measures to avoid thermal side effects (e.g. skin overheating), the required accuracy and stability of temperature monitoring, and workflow considerations such as patient positioning and integration with imaging or treatment-planning tools. These initial requirements are then translated into system-level specifications expressed in technical terms. For HT systems, this includes compliance with the standards listed in the previous section (e.g. IEC 60601, IEC 61000, ISO 10993, IEC 62304), as well as functional limits derived from the clinical requirements.

As development progresses, the system is decomposed into subsystem, as shown in Figure 2.4, and component-level specifications describing measurable performance criteria for the amplification chain, applicators, water-circulation or cooling systems, thermometry hardware, and planning/control software. For example, signal generation requirements may include a minimum phase accuracy, amplitude accuracy, and power-output tolerances; applicator requirements may include acceptable antenna coupling (e.g. $< -20\,\mathrm{dB}$) and bolus temperature stability; thermometry requirements may include a response time $< 10\,\mathrm{s}$ and precision of $\pm 0.2\,^{\circ}\mathrm{C}$ For treatment-planning (TP) software, requirements may include verification against accepted computational benchmarks [111], including demonstration of mesh-independent temperature predictions with an uncertainty below $0.05\,^{\circ}\mathrm{C}$. QA principles are embedded at this stage by ensuring that every requirement is testable, traceable, and linked to explicit acceptance criteria such as calibration intervals, allowed sensor drift, or tolerances for EM field uniformity.

The *right branch* of the V-model mirrors the design stages with structured verification and validation. At each step, testing is repeated after integrating individual components into larger subsystems and, ultimately, into the complete system. Component-level verification confirms the performance of isolated subsystems—such as amplifier performance evaluation, antenna S-parameter measurements, electromagnetic compatibility testing, and software unit verification. When external components are procured, such as temperature sensors, component-level verification is not required because these devices must already be CE-marked. However, their correct functioning within the HT system still needs to be verified during the subsystem or system integration.

Subsystem-level verification evaluates the behaviour of combined compo-

nents, including the joint performance of amplifiers and applicators in generating phase-steered fields, the influence of electromagnetic interference on thermometry accuracy, the cooling-system stability under expected loads, and correct data exchange between the treatment-planning software and the RF control unit. System-level verification assesses the fully assembled HT device, examining electromagnetic and electrical safety, the functionality of safety interlocks, the usability of the clinical interface, and overall system performance.

The next step is system commissioning, which consists of a structured set of pre-clinical verification activities guided by QA guidelines, performed after regulatory compliance but before first clinical use. Its purpose is to ensure that the complete system operates safely, reliably, and in accordance with its intended performance specifications prescribed. This may include full end-to-end tests comparing predicted and measured temperature distributions and system performance characterization based on QA defined quality metrics. Successful commissioning confirms that the device is ready for clinical implementation.

Finally, system validation demonstrates that the device fulfils its intended use in a clinical environment. Clinical validation is performed by involving patients in a clinical study designed to confirm that the system its able to deliver its intended therapeutic effect under real treatment conditions. Validation not only verifies technical performance but also shows that the device consistently meets the clinical objectives defined at the beginning of the V-model.

In summary, the MDR provides the formal regulatory foundation for defining clear and rigorous product requirements concerning safety. QA guidelines, in turn, provide clinically oriented verification procedures that ensure system reliability and clinical validity. For HT system development, integrating these two dimensions is indispensable. Only by aligning MDR-driven requirements with QA-driven verification can a system be designed that fulfils its clinical purpose, operates safely for patients and staff, and integrates smoothly into the clinical environment.

In this chapter, we clarified the relationship between the MDR and QA. Building on this, Paper E provides practical guidance for applying the MDR pathway to HT systems, supporting the development of clinically effective and regulatory-compliant technologies.

CHAPTER 6

Summary of included papers

This chapter provides a summary of the included papers.

6.1 Paper A

Mattia De Lazzari, Anna Ström, Laura Farina, Nuno P Silva, Sergio Curto, Hana Dobšíček Trefná
Ethylcellulose-stabilized fat-tissue phantom for quality assurance in clinical hyperthermia
Published in International Journal of Hyperthermia,
vol. 40, no. 1, pp. 2207797, May 2023.
 DOI: 10.1080/02656736.2023.2207797.

This paper introduces an innovative formulation for a fat-mimicking phantom material designed for use in superficial HT QA procedures. The phantom is based on an ethylcellulose (EC) stabilized glycerol-in-oil emulsion. In contrast to previously proposed fat phantoms, the formulation contains no water, which greatly simplifies the preparation process and significantly extends shelf life by preventing dehydration and microbial degradation. Moreover, the EC-

based oleogel structure provides enhanced mechanical stability, thereby addressing common limitations of earlier phantoms such as insufficient rigidity, poor handling properties, and rapid structural deterioration. The dielectric, thermal, and rheological properties of the phantom were rigorously assessed through state of the art techniques. Our phantom exhibits representative thermal and mechanical properties, able to withstand high temperatures without weakening its structure. It accurately replicates the dielectric properties of average fat tissue in the frequency range of 200–700 MHz. Moreover, reducing the glycerol concentration to 52 wt% effectively brings the conductivity within the desired range for frequencies above 700 MHz. However, the phantom conductivity is below the desired values at lower frequencies (8–200 MHz). Unfortunately, no practical solution has been identified to address the low conductivity observed at frequencies below 200 MHz, despite attempts involving the addition of salts like sodium chloride or calcium chloride. Nevertheless, the impact of this reduced conductivity was evaluated in silico for capacitive systems using numerical simulations. The results showed that the standard quality-metric parameters TEFS and TEPD were overestimated by only 13.7% and 23.5%, respectively. These findings underline the need for experimental verification on capacitive systems to confirm the numerical predictions. Finally, our phantom underwent testing for compliance with QA guidelines for superficial HT. The experimental results affirm the suitability of our phantom for routine use in superficial HT QA procedures.
Contributions. *Conceptualization:* M.D. and H.D.T.; *Methodology*: M.D., A.S.; *Formal analysis*: M.D.; *Data curation:* M.D; L.F., N.P.S.; *Writing:* M.D, A.S; *Review:* M.D, H.D.T, S.C.; *Supervision:* H.D.T.

6.2 Paper B

Mattia De Lazzari, Hana Dobšícek Trefná, Carolina Carrapiço-Seabra, Patrick V. Granton, Sergio Curto, Dario B. Rodrigues
Quality Assurance Phantoms for Deep Hyperthermia Devices: Design Principles Informed by Computational Modeling
Submitted to Physics in Medicine and Biology.

This paper investigates the design of QA phantoms for DHT devices through a combined computational and experimental approach. Parametric simula-

tions were performed using simplified models of the BSD2000 Sigma 60 applicator at 75 and 100 MHz to study the influence of phantom geometry (diameter, length, wall thickness) and dielectric properties (permittivity, conductivity) on specific absorption rate (SAR) and temperature distributions. The analysis demonstrated that conductivity has the strongest impact, with lower values improving gradient sharpness and reducing peripheral hotspots. Two cylindrical phantom designs (25 and 31.5 cm diameter) were tested, and catheter placement was optimized to maximize resolution of temperature gradients. Comparisons with anatomical patient models showed good agreement in the central regions, while deviations near the boundaries reflected the simplified phantom geometry. Experimental validation with a tissue-mimicking gel phantom confirmed the simulation predictions, with discrepancies of 0.7 $\pm$ 0.5 °C at the focus, largely explained by probe positioning errors, catheter bending, and phantom misalignment. Accounting for these effects in the simulations improved agreement and highlighted the need for positioning margins along and perpendicular to the probe axis. Overall, this study provides a validated modeling framework and practical design recommendations for phantom dimensions, material properties, and catheter placement, thereby strengthening the technical foundation for standardized, temperature-based QA of DHT applicators and supporting consistent performance assessment across clinical centers.

Contributions. *Conceptualization:* M.D., D.B.R.; *Methodology*: M.D., C.C.S. and D.B.R.; *Formal analysis*: M.D.; *Data curation:* M.D.; *Writing:* M.D.; *Review:* M.D., D.B.R. H.D.T. and S.C.; *Supervision:* D.B.R. and H.D.T.

6.3 Paper C

Carolina Carrapiço-Seabra*, **Mattia De Lazzari***, Abdelali Ameziane, Gerard C. van Rhoon, Hana Dobšícek Trefná, Sergio Curto
Application of the ESHO-QA guidelines for determining the performance of the LCA superficial hyperthermia heating system
Published in International Journal of Hyperthermia,
vol. 40, no. 1, pp. 2272578, Oct. 2023.
 DOI: 10.1080/02656736.2023.2272578
**shared first authorship.*

This paper evaluates the performance of the Lucite Cone Applicator (LCA) used in superficial HT treatments, assessing its compliance with the QA guidelines for superficial hyperthermia. Six different antenna elements were examined individually, as well as in 2×1 and 2×2 array configurations. Each antenna setup was tested by measuring the temperature distribution within a fat–muscle layered phantom manufactured according to guideline recommendations. The resulting temperature distributions were used to verify compliance with the Temperature Rise (TR) criterion and to evaluate two essential quality metrics: the Thermal Effective Field Size (TEFS) and the Thermal Effective Penetration Depth (TEPD). All LCAs fulfilled the TR requirement, producing a temperature increase greater than 6 °C at a depth of 2 cm in the phantom. The work went beyond the sole LCA QA evaluation, comparing the experimental results with simulations conducted using a standard phantom model and a realistic model segmented from CT imaging data. The mean negative difference between simulated and experimental data was 1.3°C when employing the standard phantom model, which was reduced to a mean negative difference of 0.4°C when using the realistic model. Simulated and measured TEPD exhibited good agreement for both scenarios, while some disparities were observed for TEFS. These results underline how various uncertainties during QA procedures, such as antenna positioning, applicator efficiency, water bolus utilization, and heat transfer coefficients can impact on the experiment reproducibility. It suggests that further characterization of these parameters can improve the accuracy of QA assessments. Finally, this work provided important insights from the practical application of the superficial HT guidelines—particularly regarding phantom design, fabrication, and experimental setup preparation.

Contributions. *Conceptualization:* M.D., C.C.S. (shared first authors), H.D.T. and S.C. (shared last authors); *Methodology*: M.D., C.C.S., A.A.; *Formal analysis*: M.D. and C.C.S.; *Data curation:* M.D and C.C.S.; *Writing:* M.D and C.C.S.; *Review:* M.D, C.C.S., H.D.T., S.C. and G.V.R.; *Supervision:* H.D.T, S.C. and G.V.R.

6.4 Paper D

Mattia De Lazzari*, Carolina Carrapiço-Seabra*, Dietmar Marder, Gerard C. van Rhoon, Sergio Curto, Hana Dobšícek Trefná
Toward enhanced quality assurance guidelines for deep hyperthermia devices: a multi-institution study
Published in International Journal of Hyperthermia,
vol. 41, no. 1, pp. 2436005, Nov. 2024
 DOI: 10.1080/02656736.2024.2436005
**shared first authorship.*

This paper reports on a multi-institutional evaluation of deep HT applicators, aiming to verify the feasibility of the upcoming QA protocols and allowing an inter-institutional comparison of applicator performances. Six European centers participated in the study. We performed standardized heating experiments on cylindrical phantoms equipped with catheter arrays for temperature monitoring. BSD-Sigma 60 and Sigma Eye applicators were tested by applying the same experimental protocol (10 min heating time at 1000 W). The analysis focused on three temperature-based quality metrics: overall temperature rise (TR), focus location, and focus symmetry. A total of 54 measurements were performed, of which 43 fulfilled the inclusion criteria. The results showed that all applicators, with a single exception, achieved the TR criterion of a ≥ 6 °C increase within 10 minutes. The heating focus was generally located within 1–2 cm of the intended target, and focus symmetry deviations were typically below 10% (≤ 0.8 °C). Minor differences between institutions were primarily attributed to limitations in thermometry accuracy rather than intrinsic applicator performance. Based on these findings, QA thresholds of ≥ 6 °C TR, ≤ 2 cm focus deviation, and $\leq 10\%$ symmetry deviation are proposed for integration in the upcoming deep HT QA guidelines. The study highlights the robustness and reproducibility of QA indicators across institutions and supports their adoption in updated guidelines, while emphasizing the importance of standardized phantoms and harmonized measurement protocols for consistent inter-institutional QA procedures.

Contributions. *Conceptualization:* M.D., C.C.S., H.D.T. and S.C. (shared last authors); *Methodology*: M.D., C.C.S., D.M.; *Formal analysis*: M.D. and C.C.S.; *Data curation:* M.D and C.C.S.; *Writing:* M.D. and C.C.S.; *Review:* M.D., C.C.S., H.D.T., S.C. and G.V.R.; *Supervision:* H.D.T, S.C. and G.V.R.

6.5 Paper E

Mattia De Lazzari, Anton Rink, Patrick V. Granton, Dario B. Rodrigues, Hana Dobšícek Trefná
Navigating EU MDR 2017/745 for in-house deep hyperthermia systems: A practical workflow and case study
To be submitted to IEEE Journal of Translational Engineering in Health and Medicine .

This paper presents a structured regulatory framework to support the in-house development and clinical use of external deep HT systems under the European Medical Device Regulation (EU MDR 2017/745), with specific focus on the exemption pathway defined in Article 5(5). Using a phased-array electromagnetic HT device as a representative case study, the work translates MDR requirements into a practical, stepwise workflow covering justification for in-house manufacture, risk classification, specification of General Safety and Performance Requirements (GSPRs), verification, validation, and post-market surveillance. The framework explicitly integrates hyperthermia-specific QA principles, highlighting how performance verification must be addressed alongside regulatory compliance. By clarifying stakeholder roles, documentation requirements, and decision points throughout the device lifecycle, the paper bridges the gap between technical development and regulatory implementation. References to the U.S. FDA framework are included to provide regulatory context and to highlight key differences in oversight approaches for HT technologies. Overall, this work provides actionable guidance to facilitate compliant innovation, strengthen QA–regulatory alignment, and support the safe clinical translation of advanced HT systems developed within academic and hospital environments.
Contributions. *Conceptualization:* M.D., H.D.T.; *Methodology*: M.D., A.R, P.V.G.; *Formal analysis*: M.D., A.R., P.V.G.; *Data curation:* M.D; *Writing:* A.R., P.V.G. and D.B.R.; *Review and Editing:* M.D., A.R., P.V.G., D.B.R. and H.D.T.; *Supervision:* D.B.R. and H.D.T.

CHAPTER 7

Concluding Remarks and Future Outlook

This thesis focuses on the development and implementation of QA guidelines in clinical HT. Chapter 3 introduces the tools required for QA (primarily phantoms) while Chapter 4 demonstrates how these guidelines can be translated into experimental practice. Chapter 5 then situates QA within the broader framework of the Medical Device Regulation (MDR). Collectively, these results support QA procedures for both superficial and deep HT and introduce refinements that enhance their applicability and clinical relevance, ultimately contributing to a smoother and more consistent adoption of QA protocols across HT centres.

Despite these contributions, the consistent implementation of QA guidelines across institutions remains limited. As shown in Chapter 4, even when QA protocols are available, their application varies considerably between centres. For superficial HT, temperature-based QA protocols have existed for eight years [32], yet their adoption has been limited. Our study (Paper C) offers the first fully documented execution of these guidelines. For deep HT, practices also vary widely between centres, and interpretation of existing guidance remains inconsistent—although new QA protocols are forthcoming and are expected to support a more uniform implementation. This variability cur-

rently restricts the inter-institutional comparison of HT devices performance, which would otherwise promote improved treatment quality.

To address some of these gaps, this thesis translates QA recommendations into validated, step-by-step procedures. Nonetheless, integrating QA procedures into clinical workflows remains demanding. QA activities are time-consuming, requiring extensive preparation (e.g., phantom construction as shown in Paper C) and repeated measurements, which call for optimized planning to align with clinical throughput and staff availability. Many centres also lack sufficient HT expertise and specialised equipment—such as dielectric and thermal measurement systems and well-characterised phantoms—hindering standardisation efforts. Substantial inter-institutional variability further complicates implementation, as differences in applicator performance, thermometry accuracy and calibration can produce divergent results even under nominally identical protocols, as highlighted in Paper D.

The question is now how to strengthen and support the broader adoption of QA practices. A first essential step is the creation of consensus among centres, with the explicit aim of standardising procedures, tools and acceptance criteria. A positive example is provided by the Swiss Hyperthermia Network [139], which has begun coordinating national-level efforts to define and harmonise QA procedures, leveraging the expertise of research-oriented centres to support others. A similar initiative was undertaken by the Hellenic Association of Medical Physicists [140], which proposed a standardised QA protocol aligned with ESHO recommendations.

A second area for improvement is the refinement of current guidelines. This thesis contributes by supplying practical guidance not originally included in the QA protocols. For superficial HT, we show that system characterisation should not rely solely on temperature measurements but must also include antenna efficiency, rigorous and reproducible antenna positioning, and verification of water-bolus uniformity. While we propose a practical recipe for preparing fat-equivalent phantoms, achieving highly reproducible and standardised phantoms remains challenging. Progress is being made—for instance, Kanagaratnam et al. [141] recently introduced an improved muscle phantom formulation based on the original superstuff mixture. This formulation offers long shelf life and a simplified preparation process, thereby reducing preparation time and minimizing the potential for user-induced errors.

For deep HT, we demonstrate the fundamental role of accurate thermom-

etry. Mapping inaccuracies were identified as one of the dominant sources of error in deep-HT QA. Proper calibration and verification of probes prior to QA measurements are then fundamental, as mapping errors can introduce deviations of up to 2 °C in measured temperature profiles (Paper B). Reducing these uncertainties may allow these margins to be narrowed. Therefore, we proposed a standardized procedure for systematic verification of thermal mapping devices. This, together with the reproducible positioning of phantoms are essential for obtaining reliable and comparable data across institutions. Accounting for these limitations, we proposed acceptability thresholds for deep-HT QA evaluations (see Chapter 4) that include a wider margin of deviation to accommodate potential measurement uncertainties not directly related to heating performance.

Another important consideration is the distinction between a full system characterisation and routine functionality checks. A full characterisation requires comprehensive measurements and complex phantom setups and should thus be performed periodically or when routine verification indicates irregularities. Routine checks, by contrast, should rely on simplified, time-efficient procedures that minimize the burden on clinical centres For deep HT systems, options include LED- or lamp-based phantoms, which allow rapid visual assessment of heating patterns and can reveal major applicator or coupling issues without the need for full thermal measurements. The same principle applies to superficial HT, where IR cameras can be used to quickly assess the temperature distribution. Additionally, electric-field measurements offer complementary information for both superficial and deep HT and can further support routine QA activities. While absolute E-field dosimetry remains technically demanding—due to field perturbation, dielectric loading, and calibration challenges—relative E-field measurements can still reliably detect system drift, verify steering behaviour, and assess reproducibility [142]. Recent developments, such as multi-axis E-field sensors composed of three orthogonal probes [143], represent promising steps toward more quantitative electromagnetic characterisation, although limitations related to isotropy, perturbation and scanning time still restrict their clinical practicality.

In conclusion, the translation of QA protocols into routine practice is feasible but requires further technical refinement and, above all, strong commitment from clinical centres. Establishing consensus, standardising procedures and tools, and embedding QA into the broader clinical culture are essential

to elevate hyperthermia to a new level of quality and reproducibility. The results and methodologies developed in this thesis aim to support this transition and contribute to the ongoing effort toward harmonised, reliable and clinically meaningful QA in hyperthermia.

References

[1] J. Ferlay, M. Ervik, F. Lam, *et al.*, *Global Cancer Observatory: Cancer Today*, `https://gco.iarc.who.int/today`, version 1.1, Accessed: 13 December 2025, Lyon, France, 2024.

[2] World Health Organization, *Cancer*, `https://www.who.int/news-room/fact-sheets/detail/cancer`, Fact sheet. Accessed: 13 December 2025, Feb. 2022.

[3] K. D. Miller, L. Nogueira, T. Devasia, *et al.*, "Cancer treatment and survivorship statistics, 2022," *CA: a cancer journal for clinicians*, vol. 72, no. 5, pp. 409–436, 2022.

[4] D. T. Debela, S. G. Muzazu, K. D. Heraro, *et al.*, "New approaches and procedures for cancer treatment: Current perspectives," *SAGE open medicine*, vol. 9, p. 20 503 121 211 034 366, 2021.

[5] M. Horsman and J. Overgaard, "Hyperthermia: A potent enhancer of radiotherapy," *Clinical oncology*, vol. 19, no. 6, pp. 418–426, 2007.

[6] R. D. Issels, "Hyperthermia adds to chemotherapy," *European journal of cancer*, vol. 44, no. 17, pp. 2546–2554, 2008.

[7] C. Vernon, J. Hand, S. Field, D. Machin, and J. Whaley, "Radiotherapy with or without hyperthermia in the treatment of superficial localized breast cancer: Results from five randomized controlled trials. international collaborative hyperthermia group," *International Journal of Radiation Oncology* Biology* Physics*, vol. 35, pp. 731–744, 1996.

[8] R. D. Issels, L. H. Lindner, J. Verweij, *et al.*, "Neo-adjuvant chemotherapy alone or with regional hyperthermia for localised high-risk soft-tissue sarcoma: A randomised phase 3 multicentre study," *The Lancet oncology*, vol. 11, no. 6, pp. 561–570, 2010.

[9] R. D. Issels, L. H. Lindner, J. Verweij, *et al.*, "Effect of neoadjuvant chemotherapy plus regional hyperthermia on long-term outcomes among patients with localized high-risk soft tissue sarcoma: The eortc 62961-ESHO 95 randomized clinical trial," *JAMA oncology*, vol. 4, no. 4, pp. 483–492, 2018.

[10] J. van der Zee, D. González, G. C. van Rhoon, J. D. van Dijk, W. L. van Putten, and A. A. Hart, "Comparison of radiotherapy alone with radiotherapy plus hyperthermia in locally advanced pelvic tumours: A prospective, randomised, multicentre trial," *The Lancet*, vol. 355, no. 9210, pp. 1119–1125, 2000.

[11] Y. Harima, T. Ohguri, H. Imada, *et al.*, "A multicentre randomised clinical trial of chemoradiotherapy plus hyperthermia versus chemoradiotherapy alone in patients with locally advanced cervical cancer," *International Journal of Hyperthermia*, vol. 32, no. 7, pp. 801–808, 2016.

[12] R. Issels, L. Lindner, P. Wust, *et al.*, "Regional hyperthermia (rht) improves response and survival when combined with systemic chemotherapy in the management of locally advanced, high grade soft tissue sarcomas (sts) of the extremities, the body wall and the abdomen: A phase iii randomised pros," *Journal of Clinical Oncology*, vol. 25, no. 18_suppl, pp. 10 009–10 009, 2007.

[13] E. L. Jones, T. V. Samulski, M. W. Dewhirst, *et al.*, "A pilot phase ii trial of concurrent radiotherapy, chemotherapy, and hyperthermia for locally advanced cervical carcinoma," *Cancer*, vol. 98, no. 2, pp. 277–282, 2003.

[14] N. R. Datta, E. Puric, D. Klingbiel, S. Gomez, and S. Bodis, "Hyperthermia and radiation therapy in locoregional recurrent breast cancers: A systematic review and meta-analysis," *International Journal of Radiation Oncology* Biology* Physics*, vol. 94, no. 5, pp. 1073–1087, 2016.

[15] D. F. De Haas-Kock, J. Buijsen, M. Pijls-Johannesma, *et al.*, "Concomitant hyperthermia and radiation therapy for treating locally advanced rectal cancer," *Cochrane Database of Systematic Reviews*, no. 3, 2009.

[16] A. Vasanthan, M. Mitsumori, J. H. Park, *et al.*, "Regional hyperthermia combined with radiotherapy for uterine cervical cancers: A multiinstitutional prospective randomized trial of the international atomic energy agency," *International Journal of Radiation Oncology* Biology* Physics*, vol. 61, no. 1, pp. 145–153, 2005.

[17] N. R. Datta, E. Stutz, S. Gomez, and S. Bodis, "Efficacy and safety evaluation of the various therapeutic options in locally advanced cervix cancer: A systematic review and network meta-analysis of randomized clinical trials," *International Journal of Radiation Oncology* Biology* Physics*, vol. 103, no. 2, pp. 411–437, 2019.

[18] P. W. Chiu, A. C. Chan, S. Leung, *et al.*, "Multicenter prospective randomized trial comparing standard esophagectomy with chemoradiotherapy for treatment of squamous esophageal cancer: Early results from the chinese university research group for esophageal cancer (cure)," *Journal of gastrointestinal surgery*, vol. 9, pp. 794–802, 2005.

[19] N. R. Datta, S. Rogers, S. G. Ordóñez, E. Puric, and S. Bodis, "Hyperthermia and radiotherapy in the management of head and neck cancers: A systematic review and meta-analysis," *International Journal of Hyperthermia*, vol. 32, no. 1, pp. 31–40, 2016.

[20] P. D. Veltsista, E. Oberacker, A. Ademaj, *et al.*, "Hyperthermia in the treatment of high-risk soft tissue sarcomas: A systematic review," *International Journal of Hyperthermia*, vol. 40, no. 1, p. 2 236 337, 2023.

[21] J. Overgaard, S. Bentzen, D. G. Gonzalez, *et al.*, "Randomised trial of hyperthermia as adjuvant to radiotherapy for recurrent or metastatic malignant melanoma," *The Lancet*, vol. 345, no. 8949, pp. 540–543, 1995.

[22] C. A. Perez, B. Gillespie, T. Pajak, N. B. Hornback, D. Emami, and P. Rubin, "Quality assurance problems in clinical hyperthermia and their impact on therapeutic outcome: A report by the radiation therapy oncology group," *International Journal of Radiation Oncology* Biology* Physics*, vol. 16, no. 3, pp. 551–558, 1989.

[23] J. R. Oleson, T. V. Samulski, K. A. Leopold, *et al.*, "Sensitivity of hyperthermia trial outcomes to temperature and time: Implications for thermal goals of treatment," *International Journal of Radiation Oncology* Biology* Physics*, vol. 25, no. 2, pp. 289–297, 1993.

[24] M. Sherar, F.-F. Liu, M. Pintilie, *et al.*, "Relationship between thermal dose and outcome in thermoradiotherapy treatments for superficial recurrences of breast cancer: Data from a phase iii trial," *International Journal of Radiation Oncology* Biology* Physics*, vol. 39, no. 2, pp. 371–380, 1997.

[25] A. Bakker, J. van der Zee, G. van Tienhoven, H. P. Kok, C. R. Rasch, and H. Crezee, "Temperature and thermal dose during radiotherapy and hyperthermia for recurrent breast cancer are related to clinical outcome and thermal toxicity: A systematic review," *International Journal of Hyperthermia*, vol. 36, no. 1, pp. 1023–1038, 2019.

[26] E. L. Jones, J. R. Oleson, L. R. Prosnitz, *et al.*, "Randomized trial of hyperthermia and radiation for superficial tumors," *Journal of clinical oncology*, vol. 23, no. 13, pp. 3079–3085, 2005.

[27] M. Franckena, D. Fatehi, M. de Bruijne, *et al.*, "Hyperthermia dose-effect relationship in 420 patients with cervical cancer treated with combined radiotherapy and hyperthermia," *European Journal of Cancer*, vol. 45, no. 11, pp. 1969–1978, 2009.

[28] M. Kroesen, H. T. Mulder, J. M. van Holthe, *et al.*, "Confirmation of thermal dose as a predictor of local control in cervical carcinoma patients treated with state-of-the-art radiation therapy and hyperthermia," *Radiotherapy and oncology*, vol. 140, pp. 150–158, 2019.

[29] C. P. T. Valverde, A. Bakker, H. P. Kok, *et al.*, "The probability of locoregional control in patients with locoregional recurrent breast cancer treated with postoperative reirradiation and hyperthermia (radhy): A continuous thermal dose-effect relationship," *International Journal of Radiation Oncology* Biology* Physics*, 2025.

[30] P. R. Stauffer and G. C. van Rhoon, "Overview of bladder heating technology: Matching capabilities with clinical requirements," *International Journal of Hyperthermia*, vol. 32, no. 4, pp. 407–416, 2016.

[31] H. D. Trefná, H. Crezee, M. Schmidt, *et al.*, "Quality assurance guidelines for superficial hyperthermia clinical trials: I. clinical requirements," *International Journal of Hyperthermia*, vol. 33, no. 4, pp. 471–482, 2017.

[32] H. Dobšíček Trefná, J. Crezee, M. Schmidt, *et al.*, "Quality assurance guidelines for superficial hyperthermia clinical trials: Ii. technical requirements for heating devices," *Strahlentherapie und Onkologie*, vol. 193, no. 5, pp. 351–366, 2017.

[33] H. Dobšíček Trefná, M. Schmidt, G. Van Rhoon, *et al.*, "Quality assurance guidelines for interstitial hyperthermia," *International Journal of Hyperthermia*, vol. 36, no. 1, pp. 276–293, 2019.

[34] H. Dobšíček Trefná, H. Crezee, D. Marder, *et al.*, "Quality assurance guidelines for performance assessment of phased-array deep hyperthermia therapy systems," Manuscript submitted for publication in the *International Journal of Hyperthermia*, 2025.

[35] G. Delaney, S. Jacob, C. Featherstone, and M. Barton, "The role of radiotherapy in cancer treatment: Estimating optimal utilization from a review of evidence-based clinical guidelines," *Cancer: Interdisciplinary International Journal of the American Cancer Society*, vol. 104, no. 6, pp. 1129–1137, 2005.

[36] P. R. Stauffer, "Evolving technology for thermal therapy of cancer," *International Journal of Hyperthermia*, vol. 21, no. 8, pp. 731–744, 2005.

[37] P. R. Stauffer and M. M. Paulides, "Hyperthermia therapy for cancer," in *Comprehensive Biomedical Physics*, R. Bale, M. Bennett, and R. Ritchie, Eds., Amsterdam: Elsevier, 2014, pp. 115–151.

[38] K. F. Chu and D. E. Dupuy, "Thermal ablation of tumours: Biological mechanisms and advances in therapy," *Nature Reviews Cancer*, vol. 14, no. 3, pp. 199–208, 2014.

[39] M. Ahmed, L. Solbiati, C. L. Brace, *et al.*, "Image-guided tumor ablation: Standardization of terminology and reporting criteria—a 10-year update," *Radiology*, vol. 273, no. 1, pp. 241–260, 2014.

[40] S. N. Goldberg, G. S. Gazelle, and P. R. Mueller, "Thermal ablation therapy for focal malignancy: A unified approach to underlying principles, techniques, and diagnostic imaging guidance," *American journal of roentgenology*, vol. 174, no. 2, pp. 323–331, 2000.

[41] P. Prakash, "Theoretical modeling for hepatic microwave ablation," *The open biomedical engineering journal*, vol. 4, p. 27, 2010.

[42] I. C. on Non-Ionizing Radiation Protection *et al.*, "Principles for non-ionizing radiation protection," *Health physics*, vol. 118, no. 5, pp. 477–482, 2020.

[43] O. Desouky, N. Ding, and G. Zhou, "Targeted and non-targeted effects of ionizing radiation," *Journal of Radiation Research and Applied Sciences*, vol. 8, no. 2, pp. 247–254, 2015.

[44] G. Borrego-Soto, R. Ortiz-López, and A. Rojas-Martínez, "Ionizing radiation-induced dna injury and damage detection in patients with breast cancer," *Genetics and molecular biology*, vol. 38, pp. 420–432, 2015.

[45] S. Gabriel, R. W. Lau, and C. Gabriel, "The dielectric properties of biological tissues: Ii. measurements in the frequency range 10 hz to 20 ghz," *Physics in Medicine & Biology*, vol. 41, no. 11, pp. 2251–2269, 1996.

[46] E. H. Wissler, "Pennes' 1948 paper revisited," *Journal of applied physiology*, vol. 85, no. 1, pp. 35–41, 1998.

[47] Z. Vujaskovic and C. Song, "Physiological mechanisms underlying heat-induced radiosensitization," *International Journal of Hyperthermia*, vol. 20, no. 2, pp. 163–174, 2004.

[48] W. Dewey, "Interaction of heat with radiation and chemotherapy," *Cancer research*, vol. 44, no. 10_Supplement, 4714s–4720s, 1984.

[49] N. van den Tempel, M. R. Horsman, and R. Kanaar, "Improving efficacy of hyperthermia in oncology by exploiting biological mechanisms," *International Journal of Hyperthermia*, vol. 32, no. 4, pp. 446–454, 2016.

[50] A. Oei, H. Kok, S. Oei, *et al.*, "Molecular and biological rationale of hyperthermia as radio-and chemosensitizer," *Advanced drug delivery reviews*, vol. 163, pp. 84–97, 2020.

[51] S. Field and C. Morris, "The relationship between heating time and temperature: Its relevance to clinical hyperthermia," *Radiotherapy and Oncology*, vol. 1, no. 2, pp. 179–186, 1983.

[52] X. Sun, L. Xing, C. Clifton Ling, and G. C. Li, "The effect of mild temperature hyperthermia on tumour hypoxia and blood perfusion: Relevance for radiotherapy, vascular targeting and imaging," *International Journal of Hyperthermia*, vol. 26, no. 3, pp. 224–231, 2010.

[53] M. B. Lande, J. M. Donovan, and M. L. Zeidel, "The relationship between membrane fluidity and permeabilities to water, solutes, ammonia, and protons.," *The Journal of general physiology*, vol. 106, no. 1, pp. 67–84, 1995.

[54] S. Toraya-Brown and S. Fiering, "Local tumour hyperthermia as immunotherapy for metastatic cancer," *International journal of hyperthermia*, vol. 30, no. 8, pp. 531–539, 2014.

[55] J. M. Bull, "A review of immune therapy in cancer and a question: Can thermal therapy increase tumor response?" *International Journal of Hyperthermia*, vol. 34, no. 6, pp. 840–852, 2018.

[56] S. S. Evans, E. A. Repasky, and D. T. Fisher, "Fever and the thermal regulation of immunity: The immune system feels the heat," *Nature Reviews Immunology*, vol. 15, no. 6, pp. 335–349, 2015.

[57] A. L. Oei, L. E. Vriend, J. Crezee, N. A. Franken, and P. M. Krawczyk, "Effects of hyperthermia on dna repair pathways: One treatment to inhibit them all," *Radiation Oncology*, vol. 10, pp. 1–13, 2015.

[58] M. Jasin and R. Rothstein, "Repair of strand breaks by homologous recombination," *Cold Spring Harbor perspectives in biology*, vol. 5, no. 11, a012740, 2013.

[59] N. van den Tempel, C. Laffeber, H. Odijk, *et al.*, "The effect of thermal dose on hyperthermia-mediated inhibition of dna repair through homologous recombination," *Oncotarget*, vol. 8, no. 27, p. 44 593, 2017.

[60] J. Lepock, "Role of nuclear protein denaturation and aggregation in thermal radiosensitization," *International journal of hyperthermia*, vol. 20, no. 2, pp. 115–130, 2004.

[61] S. A. Sapareto and W. C. Dewey, "Thermal dose determination in cancer therapy," *International Journal of Radiation Oncology* Biology* Physics*, vol. 10, no. 6, pp. 787–800, 1984.

[62] M. W. Dewhirst, B. Viglianti, M. Lora-Michiels, M. Hanson, and P. Hoopes, "Basic principles of thermal dosimetry and thermal thresholds for tissue damage from hyperthermia," *International Journal of Hyperthermia*, vol. 19, no. 3, pp. 267–294, 2003.

[63] W. C. Dewey and C. J. Diederich, "Hyperthermia classic commentary: 'Arrhenius relationships from the molecule and cell to the clinic'," *International Journal of Hyperthermia*, vol. 25, no. 1, pp. 21–24, 2009.

[64] G. C. van Rhoon, "Is CEM43 still a relevant thermal dose parameter for hyperthermia treatment monitoring?" *International Journal of Hyperthermia*, vol. 32, no. 1, pp. 50–62, 2016.

[65] G. Schooneveldt, A. Bakker, E. Balidemaj, *et al.*, "Thermal dosimetry for bladder hyperthermia treatment. an overview," *International Journal of Hyperthermia*, vol. 32, no. 4, pp. 417–433, 2016.

[66] N. R. Datta, D. Marder, S. Datta, *et al.*, "Quantification of thermal dose in moderate clinical hyperthermia with radiotherapy: A relook using temperature–time area under the curve (auc)," *International Journal of Hyperthermia*, vol. 38, no. 1, pp. 296–307, 2021.

[67] C. Carrapiço-Seabra, S. Curto, M. Franckena, and G. C. V. Rhoon, "Avoiding pitfalls in thermal dose effect relationship studies: A review and guide forward," *Cancers*, vol. 14, no. 19, p. 4795, 2022.

[68] A. Bakker, C. P. T. Valverde, G. van Tienhoven, *et al.*, "Post-operative re-irradiation with hyperthermia in locoregional breast cancer recurrence: Temperature matters," *Radiotherapy and Oncology*, vol. 167, pp. 149–157, 2022.

[69] J. Shafiq, M. Barton, D. Noble, C. Lemer, and L. J. Donaldson, "An international review of patient safety measures in radiotherapy practice," *Radiotherapy and Oncology*, vol. 92, no. 1, pp. 15–21, 2009.

[70] Y. Chen, J. Williams, I. Ding, *et al.*, "Radiation pneumonitis and early circulatory cytokine markers," in *Seminars in radiation oncology*, Elsevier, vol. 12, 2002, pp. 26–33.

[71] H. Majeed and V. Gupta, "Adverse effects of radiation therapy," *StatPearls*, 2020, StatPearls Publishing, Treasure Island (FL).

[72] H. Omer, "Radiobiological effects and medical applications of non-ionizing radiation," *Saudi journal of biological sciences*, vol. 28, no. 10, pp. 5585–5592, 2021.

[73] J. A. D'Andrea, J. M. Ziriax, and E. R. Adair, "Radio frequency electromagnetic fields: Mild hyperthermia and safety standards," *Progress in brain research*, vol. 162, pp. 107–135, 2007.

[74] W. H. Bailey, R. Bodemann, J. Bushberg, *et al.*, "Synopsis of IEEE std C95.1™–2019 "IEEE standard for safety levels with respect to human exposure to electric, magnetic, and electromagnetic fields, 0 Hz to 300 GHz"," *IEEE Access*, vol. 7, pp. 171 346–171 356, 2019.

[75] I. C. on Non-Ionizing Radiation Protection *et al.*, "Guidelines for limiting exposure to electromagnetic fields (100 khz to 300 ghz)," *Health physics*, vol. 118, no. 5, pp. 483–524, 2020.

[76] H. P. Kok, E. N. Cressman, W. Ceelen, *et al.*, "Heating technology for malignant tumors: A review," *International Journal of Hyperthermia*, vol. 37, no. 1, pp. 711–741, 2020.

[77] M. Paulides, H. D. Trefna, S. Curto, and D. Rodrigues, "Recent technological advancements in radiofrequency-andmicrowave-mediated hyperthermia for enhancing drug delivery," *Advanced drug delivery reviews*, vol. 163, pp. 3–18, 2020.

[78] G. Van Rhoon, P. Rietveld, and J. Van der Zee, "A 433 MHz lucite cone waveguide applicator for superficial hyperthermia," *International journal of hyperthermia*, vol. 14, no. 1, pp. 13–27, 1998.

[79] P. R. Stauffer, P. Maccarini, K. Arunachalam, *et al.*, "Conformal microwave array (cma) applicators for hyperthermia of diffuse chest wall recurrence," *International Journal of Hyperthermia*, vol. 26, no. 7, pp. 686–698, 2010.

[80] H. Kok, F. Navarro, L. Strigari, M. Cavagnaro, and J. Crezee, "Locoregional hyperthermia of deep-seated tumours applied with capacitive and radiative systems: A simulation study," *International Journal of Hyperthermia*, vol. 34, no. 6, pp. 714–730, 2018.

[81] H. Kok and J. Crezee, "A comparison of the heating characteristics of capacitive and radiative superficial hyperthermia," *International Journal of Hyperthermia*, vol. 33, no. 4, pp. 378–386, 2017.

[82] M. Hiraoka, S. Jo, K. Akuta, Y. Nishimura, M. Takahashi, and M. Abe, "Radiofrequency capacitive hyperthermia for deep-seated tumors. i. studies on thermometry," *Cancer*, vol. 60, no. 1, pp. 121–127, 1987.

[83] M. Notter, H. Piazena, and P. Vaupel, "Hypofractionated re-irradiation of large-sized recurrent breast cancer with thermography-controlled, contact-free water-filtered infra-red-a hyperthermia: A retrospective study of 73 patients," *International Journal of Hyperthermia*, vol. 33, no. 2, pp. 227–236, 2017.

[84] J. van der Zee and D. González, "The Dutch deep hyperthermia trial: Results in cervical cancer," *International Journal of Hyperthermia*, vol. 18, no. 1, pp. 1–12, 2002.

[85] O. J. Ott, U. S. Gaipl, A. Lamrani, and R. Fietkau, "The emerging evidence supporting integration of deep regional hyperthermia with chemoradiation in bladder cancer," in *Seminars in Radiation Oncology*, Elsevier, vol. 33, 2023, pp. 82–90.

[86] R. Wessalowski, D. T. Schneider, O. Mils, *et al.*, "Regional deep hyperthermia for salvage treatment of children and adolescents with refractory or recurrent non-testicular malignant germ-cell tumours: An open-label, non-randomised, single-institution, phase 2 study," *The Lancet oncology*, vol. 14, no. 9, pp. 843–852, 2013.

[87] H. Kok, M. De Greef, P. Borsboom, A. Bel, and J. Crezee, "Improved power steering with double and triple ring waveguide systems: The impact of the operating frequency," *International Journal of Hyperthermia*, vol. 27, no. 3, pp. 224–239, 2011.

[88] K. D. Paulsen, S. Geimer, J. Tang, and W. E. Boyse, "Optimization of pelvic heating rate distributions with electromagnetic phased arrays," *International Journal of Hyperthermia*, vol. 15, no. 3, pp. 157–186, 1999.

[89] M. Paulides, Z. Rijnen, P. Togni, *et al.*, "Clinical introduction of novel microwave hyperthermia technology: The hypercollar3d applicator for head and neck hyperthermia," in *2015 9th European Conference on Antennas and Propagation (EuCAP)*, IEEE, 2015, pp. 1–4.

[90] P. Takook, M. Shafiemehr, M. Persson, and H. D. Trefná, "Experimental evaluation of UWB applicator prototype for head and neck hyperthermia," in *2017 11th European Conference on Antennas and Propagation (EUCAP)*, IEEE, 2017, pp. 3619–3620.

[91] T. P. Ryan and C. L. Brace, "Interstitial microwave treatment for cancer: Historical basis and current techniques in antenna design and performance," *International Journal of Hyperthermia*, vol. 33, no. 1, pp. 3–14, 2017.

[92] P. K. Sneed, P. R. Stauffer, M. W. McDermott, *et al.*, "Survival benefit of hyperthermia in a prospective randomized trial of brachytherapy boost±hyperthermia for glioblastoma multiforme," *International Journal of Radiation Oncology* Biology* Physics*, vol. 40, no. 2, pp. 287–295, 1998.

[93] C. Coughlin, E. Douple, J. Strohbehn, W. Eaton Jr, B. Trembly, and T. Wong, "Interstitial hyperthermia in combination with brachytherapy.," *Radiology*, vol. 148, no. 1, pp. 285–288, 1983.

[94] G. Lassche, J. Crezee, and C. Van Herpen, "Whole-body hyperthermia in combination with systemic therapy in advanced solid malignancies," *Critical reviews in oncology/hematology*, vol. 139, pp. 67–74, 2019.

[95] J. M. Bull, G. L. Scott, F. R. Strebel, *et al.*, "Fever-range whole-body thermal therapy combined with cisplatin, gemcitabine, and daily interferon-α: A description of a phase I-II protocol," *International Journal of Hyperthermia*, vol. 24, no. 8, pp. 649–662, 2008.

[96] International Organization for Standardization, "Quality Management Systems — Fundamentals and Vocabulary," International Organization for Standardization, Geneva, Switzerland, International Standard ISO 9000:2015, Sep. 2015.

[97] C. B. Saw, M. S. Ferenci, and H. Wanger Jr, "Technical aspects of quality assurance in radiation oncology," *Biomedical imaging and intervention journal*, vol. 4, no. 3, 2008.

[98] J. Hand, J. Lagenduk, J. B. Andersen, and J. C. Bolomey, "Quality assurance guidelines for ESHO protocols," *International Journal of Hyperthermia*, vol. 5, no. 4, pp. 421–428, 1989.

[99] J. Lagendijk, G. Van Rhoon, S. Hornsleth, *et al.*, "ESHO quality assurance guidelines for regional hyperthermia," *International Journal of Hyperthermia*, vol. 14, no. 2, pp. 125–133, 1998.

[100] M. Dewhirst, T. Phillips, T. Samulski, *et al.*, "Rtog quality assurance guidelines for clinical trials using hyperthermia," *International Journal of Radiation Oncology* Biology* Physics*, vol. 18, no. 5, pp. 1249–1259, 1990.

[101] G. Bruggmoser, S. Bauchowitz, R. Canters, *et al.*, "Quality assurance for clinical studies in regional deep hyperthermia," *Strahlentherapie und Onkologie*, vol. 187, no. 10, p. 605, 2011.

[102] D. I. Thwaites, B. J. Mijnheer, and J. A. Mills, "Quality assurance of external beam radiotherapy," in *Radiation Oncology Physics: A Handbook for Teachers and Students*, Vienna, Austria: International Atomic Energy Agency, 2005, pp. 407–450.

[103] R. J. Shalek, "Determination of absorbed dose in a patient irradiated by beams of X or gamma rays in radiotherapy procedures," *Medical Physics*, vol. 4, no. 5, p. 461, 1977.

[104] W. Van Gijn, P. Krijnen, V. Lemmens, M. Den Dulk, H. Putter, and C. van de Velde, "Quality assurance in rectal cancer treatment in the netherlands: A catch up compared to colon cancer treatment," *European Journal of Surgical Oncology (EJSO)*, vol. 36, no. 4, pp. 340–344, 2010.

[105] World Health Organization, *Quality Assurance in Radiotherapy: A Guide Prepared Following a Workshop Held at Schloss Reisensburg, Federal Republic of Germany, 3–7 December 1984*. Geneva, Switzerland: World Health Organization, 1988.

[106] G. J. Kutcher, L. Coia, M. Gillin, *et al.*, "Comprehensive QA for radiation oncology: Report of AAPM radiation therapy committee task group 40," *Medical Physics*, vol. 21, no. 4, pp. 581–618, 1994.

[107] K. Vergote, Y. De Deene, W. Duthoy, *et al.*, "Validation and application of polymer gel dosimetry for the dose verification of an intensity-modulated arc therapy (imat) treatment," *Physics in Medicine & Biology*, vol. 49, no. 2, p. 287, 2004.

[108] E. E. Klein, J. Hanley, J. Bayouth, *et al.*, "Task group 142 report: Quality assurance of medical accelerators," *Medical Physics*, vol. 36, no. 9, pp. 4197–4212, 2009.

[109] T. Pawlicki and et al., "Task group 179 report: Quality assurance for image-guided radiation therapy using ct-based technologies," *Medical Physics*, vol. 39, no. 12, pp. 6969–7000, 2012.

[110] R. A. Siochi, P. Balter, C. D. Bloch, *et al.*, "A rapid communication from the aapm task group 201: Recommendations for the QA of external beam radiotherapy data transfer. aapm tg 201: Quality assurance of external beam radiotherapy data transfer," *Journal of applied clinical medical physics*, vol. 12, no. 1, pp. 170–181, 2011.

[111] M. M. Paulides, D. B. Rodrigues, G. G. Bellizzi, *et al.*, "ESHO benchmarks for computational modeling and optimization in hyperthermia therapy," *International Journal of Hyperthermia*, vol. 38, no. 1, pp. 1425–1442, 2021.

[112] R. Canters, M. Franckena, M. Paulides, and G. Van Rhoon, "Patient positioning in deep hyperthermia: Influences of inaccuracies, signal correction possibilities and optimization potential," *Physics in Medicine & Biology*, vol. 54, no. 12, p. 3923, 2009.

[113] G. Bruggmoser, S. Bauchowitz, R. Canters, *et al.*, "Guideline for the clinical application, documentation and analysis of clinical studies for regional deep hyperthermia," *Strahlenther. Onkol*, vol. 188, pp. 198–211, 2012.

[114] M. H. Seegenschmiedt, P. Fessenden, and C. C. Vernon, *Thermoradiotherapy and Thermochemotherapy: Biology, Physiology, Physics*. Springer, 1995, vol. 1.

[115] R. J. Myerson, E. G. Moros, C. J. Diederich, *et al.*, "Components of a hyperthermia clinic: Recommendations for staffing, equipment, and treatment monitoring," *International Journal of Hyperthermia*, vol. 30, no. 1, pp. 1–5, 2014.

[116] P. Wust, H. Fähling, R. Felix, *et al.*, "Quality control of the sigma applicator using a lamp phantom: A four-centre comparison," *International Journal of Hyperthermia*, vol. 11, no. 6, pp. 755–768, 1995.

[117] S. Curto, H. T. Mulder, B. Aklan, *et al.*, "A multi-institution study: Comparison of the heating patterns of five different mr-guided deep hyperthermia systems using an anthropomorphic phantom," *International Journal of Hyperthermia*, vol. 37, no. 1, pp. 1103–1115, 2020.

[118] H. T. Mulder, S. Curto, M. M. Paulides, M. Franckena, and G. C. van Rhoon, "Systematic quality assurance of the bsd2000-3d mr-compatible hyperthermia applicator performance using mr temperature imaging," *International Journal of Hyperthermia*, vol. 35, no. 1, pp. 305–313, 2018.

[119] P. Wust, H. Fähling, A. Jordan, J. Nadobny, M. Seebass, and R. Felix, "Development and testing of SAR-visualizing phantoms for quality control in RF hyperthermia," *International Journal of Hyperthermia*, vol. 10, no. 1, pp. 127–142, 1994.

[120] P. Nilsson, "Physics and technique of microwave-induced hyperthermia in the treatment of malignant tumours.," Ph.D. dissertation, University of Lund, 1984.

[121] K. Ito, K. Furuya, Y. Okano, and L. Hamada, "Development and characteristics of a biological tissue-equivalent phantom for microwaves," *Electronics and Communications in Japan (Part I: Communications)*, vol. 84, no. 4, pp. 67–77, 2001.

[122] J. Lagendijk and P. Nilsson, "Hyperthermia dough: A fat and bone equivalent phantom to test microwave/radiofrequency hyperthermia heating systems," *Physics in medicine & biology*, vol. 30, no. 7, p. 709, 1985.

[123] H. D. Trefná, S. L. Navarro, F. Lorentzon, T. Nypelö, and A. Ström, "Fat tissue equivalent phantoms for microwave applications by reinforcing gelatin with nanocellulose," *Biomedical Physics & Engineering Express*, vol. 7, no. 6, p. 065 025, 2021.

[124] S. Allen, G. Kantor, H. Bassen, and P. Ruggera, "Quality-assurance reports: Cdrh rf phantom for hyperthermia systems evaluations," *International Journal of Hyperthermia*, vol. 4, no. 1, pp. 17–23, 1988.

[125] Y. Nikawa, M. Chino, and K. Kikuchi, "Soft and dry phantom modeling material using silicone rubber with carbon fiber," *IEEE transactions on microwave theory and techniques*, vol. 44, no. 10, pp. 1949–1953, 1996.

[126] J. Garrett and E. Fear, "Stable and flexible materials to mimic the dielectric properties of human soft tissues," *IEEE Antennas and Wireless Propagation Letters*, vol. 13, pp. 599–602, 2014.

[127] P. Hasgall, F. Di Gennaro, C. Baumgartner, *et al.*, "It'is database for thermal and electromagnetic parameters of biological tissues. version 4.0, 2018," *DOI: https://doi. org/10.13099/VIP21000-04-0. itis. swiss/database*, 2022.

[128] P. M. Meaney, C. J. Fox, S. D. Geimer, and K. D. Paulsen, "Electrical characterization of glycerin: Water mixtures: Implications for use as a coupling medium in microwave tomography," *IEEE transactions on microwave theory and techniques*, vol. 65, no. 5, pp. 1471–1478, 2017.

[129] M. De Lazzari, W. Napieralski, T. Nguyen, A. Ström, and H. D. Trefná, "Design and manufacture procedures of phantoms for hyperthermia QA guidelines," in *2023 17th European Conference on Antennas and Propagation (EuCAP)*, IEEE, 2023, pp. 1–5.

[130] R. Muratoglu, D. Gerster, J. Nadobny, *et al.*, "Comparisons of computer simulations and experimental data for capacitive hyperthermia using different split-phantoms," *International Journal of Hyperthermia*, vol. 41, no. 1, p. 2 416 999, 2024.

[131] M. M. Paulides, J. F. Bakker, A. P. Zwamborn, and G. C. Van Rhoon, "A head and neck hyperthermia applicator: Theoretical antenna array design," *International Journal of Hyperthermia*, vol. 23, no. 1, pp. 59–67, 2007.

[132] P. Takook, M. Persson, J. Gellermann, and H. D. Trefná, "Compact self-grounded bow-tie antenna design for an UWB phased-array hyperthermia applicator," *International Journal of Hyperthermia*, vol. 33, no. 4, pp. 387–400, 2017.

[133] C. Carrapiço-Seabra, M. De Lazzari, A. Ameziane, G. C. van Rhoon, H. Dobšícek Trefná, and S. Curto, "Application of the ESHO-QA guidelines for determining the performance of the LCA superficial hyperthermia heating system," *International Journal of Hyperthermia*, vol. 40, no. 1, p. 2 272 578, 2023.

[134] M. De Lazzari, C. Carrapiço-Seabra, D. Marder, G. C. van Rhoon, S. Curto, and H. Dobšíček Trefná, "Toward enhanced quality assurance guidelines for deep hyperthermia devices: A multi-institution study," *International Journal of Hyperthermia*, vol. 41, no. 1, p. 2 436 005, 2024.

[135] European Parliament and Council of the European Union, *Regulation (EU) 2017/745 of the European Parliament and of the Council on Medical Devices*, Official Journal of the European Union, L117, 5 May 2017, OJ L 117, 5.5.2017, pp. 1–175, 2017.

[136] R. Baines, P. Hoogendoorn, S. Stevens, *et al.*, "Navigating medical device certification: A qualitative exploration of barriers and enablers amongst innovators, notified bodies and other stakeholders," *Therapeutic Innovation & Regulatory Science*, vol. 57, no. 2, pp. 238–250, 2023.

[137] C. Lindholm and M. Höst, "Development of software for safety critical medical devices-an interview-based survey of state of practice," in *Software Engineering Research and Practise in Sweden (SERPS)*, 2008.

[138] W. W. Royce, "Managing the development of large software systems," *Proceedings of IEEE WESCON*, pp. 1–9, 1970.

[139] E. Stutz, E. Puric, A. Ademaj, *et al.*, "Present practice of radiative deep hyperthermia in combination with radiotherapy in switzerland," *Cancers*, vol. 14, no. 5, p. 1175, 2022.

[140] S. Triantopoulou, K. Platoni, C. Antypas, *et al.*, "Quality assurance protocol for superficial and deep hyperthermia systems established by the hellenic association of medical physicists (hamp) in cooperation with the hellenic society of oncologic hyperthemia (hsoh): A study based on european society for hyperthermic oncology (ESHO) quality assurance guidelines.," *Journal of BU ON.: Official Journal of the Balkan Union of Oncology*, vol. 23, no. 2, pp. 494–499, 2018.

[141] A. Kanagaratnam, C. Carrapiço-Seabra, and S. Curto, "Muscle equivalent tissue material for superficial hyperthermia quality assurance," in *Proceedings of the European Society for Hyperthermic Oncology (ESHO)*, Conference abstract, 2024.

[142] J. Groen, R. Zweije, J. Sijbrands, *et al.*, "Presentation and characterisation of the alba micro8 system for targeted hyperthermia in small animal research," *Scientific Reports*, vol. 15, no. 1, p. 37 885, 2025.

[143] M. Di Cristofano, L. Lalli, G. Paglialunga, and M. Cavagnaro, "Electric field measurement in radiative hyperthermia applications," *Sensors*, vol. 25, no. 14, p. 4392, 2025.